

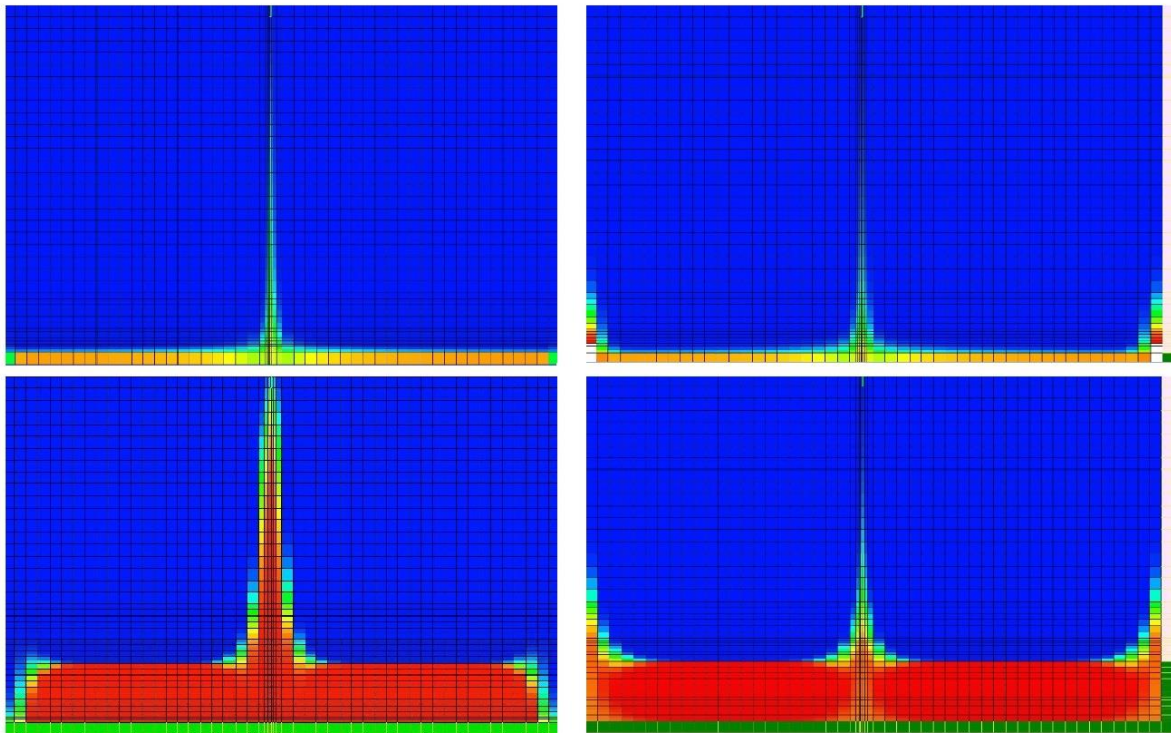


Universiteit Utrecht



Modelling saline water migration during dewatering of excavation sites; the role of density-driven flow during risk-assessments of upwelling saline water

MSc. Thesis



Earth Sciences – Utrecht University – CRUX Engineering

Author:	Carl Geuljans (6036708)	c.e.geuljans@students.uu.nl
Supervisor Utrecht University:	Prof. dr. Ruud Schotting	schotting.ruud@gmail.com
Supervisor CRUX engineering:	Dr. Thomas Sweijen	sweijen@cruxbv.nl

Final version; 27-02-2019: MSc Thesis, Earth Sciences, Universiteit Utrecht

Abstract

In coastal areas, aquifer salinization is a major risk during large-scale dewatering operations. This risk is enhanced when extraction wells are used to pump large amounts of water from coastal aquifers. Underneath an extraction well, the salt-fresh water interface may rise towards the surface. To prevent salinization of the sub-soil, the rising salt cone needs to be analyzed, and quantified. To predict the amount and extent of the saline water rise, multiple numerical and analytical methods are available. This report will assess analytical and numerical solutions to solve this problem, and to review which method suits best for each operation. To solve the numerical solutions, a modelling study will be carried out using the MODFLOW code, and MODFLOW extensions: MT3DMS and SEAWAT2000 v4. These methods will be compared with a focus on (1) the role of density-dependent flow and (2) the effects of dispersion to the mixing zone. A method will be provided that uses the numerically light MT3DMS code to predict results of the numerically heavier SEAWAT2000 v4 model. Using this method, time can be spared when assessing whether the risk of salinization is significant or not. A correction factor for the MT3DMS model results can be applied, which is dependent on the vertical distance of the saline water to the extraction well.

Table of Contents	3
1. Introduction	4
1.1. Background information	4
1.2. Problem definition	5
1.3. History of numerical modelling	6
2. Methodology	9
2.1. Conceptual model	9
2.2. Modelling methods	10
2.3. Parameterization	11
2.3.1. Default scenario	11
2.3.2. Sensitivity analysis: Modelling tracer transport	12
2.4. Analysis of MT3DMS and SEAWAT2000 v4	13
2.4.1. New method: MT3DMS corrected	13
3. Results and Discussion	15
3.1. Tracer transport with MT3DMS	15
3.1.1. Pumping time	15
3.1.2. Sensitivity analysis	17
3.2. Tracer transport vs density-dependent flow	23
3.2.1. General results	23
3.2.2. Results MT3DMS corrected	23
3.2.3. Vertical extent of the salt cone	24
3.2.4. Concentration of the recovered water	26
3.2.5. Effect of salt availability on upconing	27
3.3. Comparison of numerical models to analytical solutions	29
3.3.1. Radial flow equation	29
3.3.2. Analytical solution of Mercado (1969)	30
3.3.3. Analytical solution of Dagan and Bear (1968)	32
4. Conclusion	34
4.1. Summary different models	34
4.2. Practical applications	36
4.3. Recommendations	37
5. References	39
6. Appendix	43
6.1. Henry problem (1968)	43
6.2. Determining numerical dispersion	44

Chapter 1: Introduction

1.1 Background information

In coastal areas of the Netherlands (Figure 1.1), groundwater processes in the subsurface are mostly governed by the proximity to the sea. One of the consequences, is the intrusion of saline water into fresh water aquifers underneath both urban and rural areas. Between the fresh and salt water, an interface exists, with fresh water on top of denser saline water. This interface is not a sharp interface, but rather a diffuse interface. This means that there is an area of mixed brackish water, that ranges from centimetres to meters in thickness. In general, the larger the distance to the coast, the deeper this interface will be (Figure 1.1). However, due to anthropogenic interference with the groundwater, the salt-fresh water interface is able to rise to the surface (Oude Essink, 2001; Oude Essink et al., 2010; Bear et al., 1999; De Lange et al., 2014). Rising salt water causes **salinization** of shallow aquifers and subsoils and might cause significant damage to crops and plants in both nature and agriculture, infrastructure and drinking water reservoirs (Dehaan & Taylor, 2002).

To protect fresh water aquifers, the Dutch government has imposed regulations on the amount of soil salinization that is allowed. Salinization can occur as a result of rising saline water. This saline water is able to rise as a result of large-scale pumping events during dewatering operations. Large dewatering operations are necessary for various reasons, during engineering projects, projects by the regional water authorities or other governmental projects. Engineering companies often need to create large-scale excavation pits for construction projects. These companies are required to perform a **risk assessment** to evaluate the risk of salinization. In other words, prior to large-scale pumping events, the risk of extracting salt or brackish water needs to be assessed in order to prevent net transport of salt to the surface.

During the excavation of construction pits, phreatic and non-phreatic groundwater is extracted and large amounts of soil and subsurface are removed in order to develop the foundations of buildings. The objective of the dewatering operation is to: (1) lower the water table and intercept seepage which would otherwise enter the excavation, (2) improve the vertical stability of slopes and prevent slippages, (3) prevent ruptures, heave and liquefaction of the bottom surface of the building pit, and (4) reduce lateral pressures on temporary sheeting and bracing (Puller, 2003)

The removal of overburden weight leads to a relative overpressure inside underlying aquifers. To prevent ruptures and liquefaction in the bottom surface of the building pit, the water pressure in the underlying aquifer is lowered by extracting water from this layer. This process is called Artesian Pressure Reduction

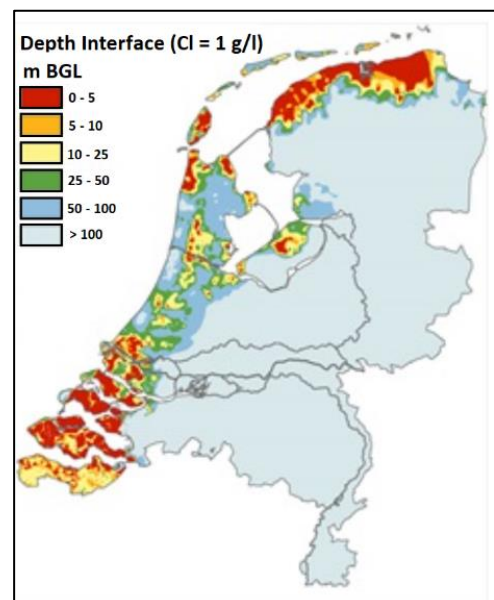


Figure 1.1: Western and northern parts of the Netherlands have areas with a very shallow salt-fresh water interface. In particular Zeeland, North Noord-Holland and North Friesland and Groningen are prone to shallow interfaces (De Louw et al., 2013).

with the use of pressure relief wells (in Dutch: spanningsbemaling) (Scott, 1983). Since the water amount that needs to be removed can be large, the chance of upwelling saline water is significant.

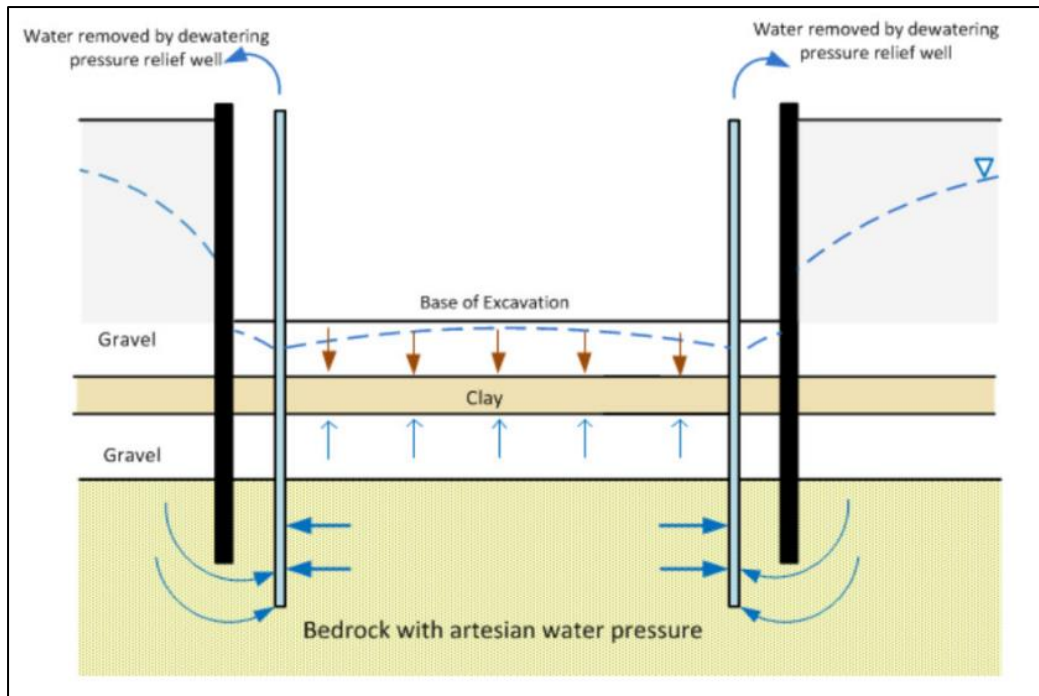


Figure 1.2: Schematic representation of an excavation pit with 2 pressure relief wells. Extracting water from the underlying aquifer reduces the groundwater uplift pressure to less than the weight of the overlying soil to prevent cracks, heave and liquefaction. This extraction can thus create an upwelling of brackish water towards the surface, if the salt-fresh water interface is shallow enough. <http://www.oqi.co.uk/artesian-pressure->

This research primarily focuses on the Dutch subsurface. However, its findings can be applied to many more locations. The Dutch (sub)surface currently faces risks (flooding and salinization) which is becoming a major issue for other lowland coastal areas (Oude Essink et al., 2010) such as the Mekong, Ganges, Mississippi and the Po river deltas. (Barlow & Reichard, 2010; Custodio, 2010; Giambastiani et al., 2007; Ranjan et al., 2006).

1.2 Problem definition

An extraction well may cause a rise of an underlying salt-fresh water interface, if saline water is present in the same aquifer as the extraction well. To predict the level of saline water rise, multiple numerical and analytical methods are available. This report will assess both the analytical and the numerical solutions to solve this problem. To solve the numerical solutions, a **modelling study** will be carried out using the MODFLOW code (McDonald and Harbaugh, 1988; Harbaugh et al. 2000), in which the salt will be modelled as a solute. Solute transport modelling can be conducted using **two different methods**. The first method uses the MODFLOW extension of **MT3DMS** (Zheng & Wang, 1999), to model the movement of the salt as a tracer. This method has a fast computing time but neglects the density difference between fresh and salt water. The second method is the numerically heavier model **SEAWAT2000 v4** (Langevin et al. 2008). This method is more accurate since it does consider **density differences**, but the extra complexity causes a greater computational load for large groundwater systems.

MT3DMS and SEAWAT2000 v4 operate differently in a numerical sense (Figure 1.3). MT3DMS uses a finite-difference method to calculate the solute transport, after the constant density flow has been calculated by MODFLOW. The method used in SEAWAT2000 v4 calculates the head after every time step and corrects for the density difference in every time step, so the density-dependent solute transport calculations have to be carried out in every time step. These corrected values of the heads and fluxes are reviewed by MODFLOW, and new values are created for the next timestep. This numerical complexity leads to a substantially longer model runtime.

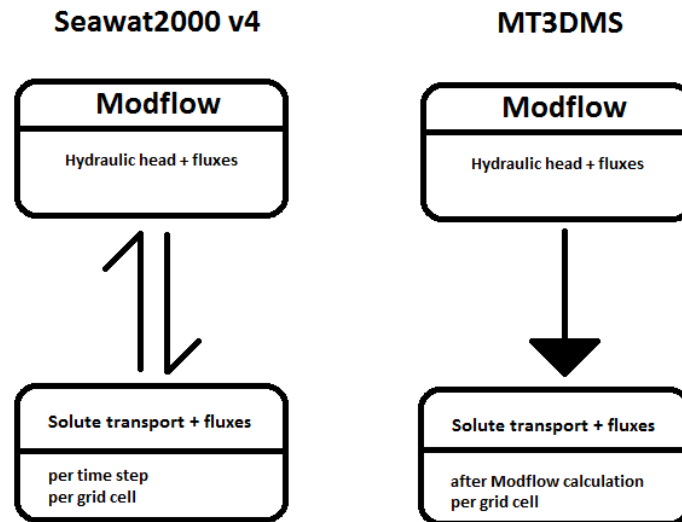


Figure 1.3: Schematic representation of the numerical difference between SEAWAT2000 v4 and MT3DMS. During the calculation of SEAWAT2000 v4, the hydraulic head and fluxes are updated per time step and per grid cell. This updated value is based on the effects of the heavier saline water to the hydraulic head. MT3DMS does not consider this effect, thus, it only needs to calculate solute transport once.

One of the **main goals** of the research is to provide a method that uses the computationally light MT3DMS model, but that produces results that resemble the results of the SEAWAT2000 v4 calculation. As such, an estimation of the error can be given in order to quantify the difference between these two models. The effects of physical and numerical dispersivity on the development of the mixing zone was studied, in combination with the role of density-dependent flow. The research will start with considering one extraction well, where MT3DMS and SEAWAT are compared under different conditions, by varying parameters such as the duration of pumping time, hydraulic conductivity, depth of the fresh/salt interface, pumping rate, etc. From these simulations, an insight can be gained into the difference between the two models. Afterwards, a comparison to three analytical solutions will be made in order to verify the modelling results of MT3DMS and SEAWAT2000 v4. Two of these analytical solutions are that of Mercado (1969), and that of Dagan & Bear (1968).

The research question is: **What is the best method to determine the extent of saline water upconing beneath an extraction well?** This question is closely related to the question as to how to predict saline water migration during large-scale water extraction of confined aquifers, and what is the correction factor to apply to the results of the MT3DMS modelling method.

To study the research question, a numerical model is necessary. For this purpose, the ground water model **Groundwater Vistas** Version 7.19 (Rumbaugh & Rumbaugh, 2017) will be used to implement the

MODFLOW code and the necessary SEAWAT and MT3DMS extension. Multiple hydrogeological parameters have to be used as inputs for the model, such as: aquifer thickness, hydraulic conductivity, porosity and dispersivity. At first, theoretical input values will be used to create a basic model to perform a **sensitivity analysis** on. Then, we will investigate which hydrogeological parameters affect the model the most. Model results will be verified by comparing its results to semi-analytical solutions of the Henry problem (1964). Also, **three analytical solutions** of the hydrological equations will be examined and compared to the modelled results. Afterwards, the **effects of dispersion** will be investigated, to quantify the effects of numerical and physical dispersivity. The final step is to create a **correction method** for the MT3DMS extension as such that the results will resemble accurate saline water migration as precise possible, without the need to run the SEAWAT extension.

1.3 Previous research: History of numerical modelling

1.3.1 Tracer transport modeling

MT3D was the first advanced solute transport code tied directly to finite-difference groundwater flow model of MODFLOW by Chunmiao Zheng in 1990 at S.S. Papadopoulos & Associates (Zheng, 1990). MT3D contained wide-ranging solution options for its time, including the method of characteristics (MOC), the modified method of characteristics (MMOC), a hybrid of these two methods (HMOC), and the standard finite-difference method (FDM).

MT3DMS was released in 1999, as the successor of the transport model MT3D (Zheng & Wang, 1999). MT3DMS contained clearly extended options, including the addition of a TVD scheme; 2) an efficient iterative solver based on Generalized Conjugate Gradient (GCG) methods; 3) options for accommodating non-equilibrium sorption, and many more options (Zheng & Wang, 1998).

1.3.2 First efforts modelling density-dependent flow

Most ground water problems are solved with a numerical model in which the density is approximated as constant, like with the MODFLOW code (McDonald and Harbaugh 1988; Harbaugh et al. 2000). When the urge for a density dependent flow model grew, Guo and Bennett (1998), Oude Essink (1998), and van Gerven and Schaars (1998) tried to simulate density-dependent flow with a MODFLOW-based code coupled with an advective and dispersive transport program. They opted to apply their methods for a number of unsolved density dependent ground water problems. For example, at ground water flow near the coast where salt water intrusion and sub-marine ground water discharge needed to be simulated. Other types of ground water transport problems where fluid density plays an important role include (1) aquifer storage and recovery (ASR), (2) deep-well injection, and (3) ground water flow near salt domes. Two of these initial programs, MOCDENS3D (Oude Essink, 1998) and SEAWAT (Guo and Bennett, 1998), have been continuously updated with recent developments and adaptations, including the incorporation inside MODFLOW-2000 (Harbaugh et al., 2000). SEAWAT and MOCDENS3D have comparable approaches; the main functional difference is that MT3DMS (Zheng and Wang, 1999) is used to compute solute transport in SEAWAT, and that Ground Water Transport Process (previously referred to as MOC3D; Konikow et al., 1996) is used to calculate solute transport in MOCDENS3D.

Sorek and Pinder (1999) published an analysis of 15 computer codes that can be used to model density-driven ground water flow. Two frequently used examples are the USGS finite-element SUTRA code (Voss 1984; Voss and Provost 2002) and the finite-difference HST3D code (Kipp Jr, K. L., 1986). Two additional MODFLOW-based programs are currently available for simulation of density-driven groundwater

transport: MODHMS (HydroGeoLogic Inc., 2002) and the SWI Package for MODFLOW (Bakker M., 2003). MODHMS is comparable to SEAWAT and MOCDENS3D for the fact that it models dispersion in solute transport, while the SWI extension provides a non-dispersive, constant flow approach to model the movement of variable-density interfaces. In the publication of (Langevin et al., 2004) these MODFLOW-based density-dependent codes are summarized.

All codes of MODFLOW until the year 2000 were designed to model variable-density groundwater transport using a formulation of the ground water flow equation in terms of equivalent fresh water head. With this fresh water head computation, density effects could be combined into a constant-density flow model described by Lebbe (1983). He similarly applied an equivalent fresh water head formulation of the flow equation by adjusting the technique of characteristics program (Konikow and Bredehoeft, 1978) to model variable-density flow. With the exclusion of the methods by Lebbe (1983) and Olsthoorn (2000), which used a two-dimensional system, a restriction with these previous methods was that a known density field was needed before the simulation, in order to calculate the heads. Also, the density field was assumed to remain constant during the simulation. Methods and approaches for studying variable-density ground water flow are summarized by Simmons et al. (2001), Diersch and Kolditz (2002), Post (2005), Simmons (2005) and Langevin & Guo (2006).

1.3.3 Density-dependent flow modeling with SEAWAT

SEAWAT2000 Version 4 was released by the U.S. Geological Survey in 2008 (Langevin et al., 2008), and is the version which is used for this modelling study. SEAWAT2000 Version 4 calculates variable-density ground-water flow coupled with multi-species solute and heat transport and keeps all of the functionalities of SEAWAT-2000 (Langevin et al., 2008). SEAWAT2000 Version 4 also contains new simulation options for coupling flow and transport, and for representing constant-head boundaries. Previous versions of SEAWAT solved the flow equation for every transport time step, regardless of whether or not there was a significant change in fluid density. Another option was applied in SEAWAT2000 Version 4 that lets users determine how many times the grid is updated. More options were also added for representing constant-head boundaries with the Time-Variant Constant-Head (CHD) Package. These options greatly increase the flexibility in the CHD flow boundaries along with non-dispersive flux solute boundaries applied by MT3DMS at constant-head cells (Langevin et al., 2008).

2. Methodology

2.1 Conceptual model

To model the rise of saline water, we use a scenario that represents a real-world scenario with a single extraction well in a three-dimensional space (Figure 2.1). This extraction well is placed at the top of a consolidated sandy aquifer. This means that the top and bottom of the aquifer are considered to be impermeable layers, through which water flow is impossible. The sides of the aquifer are not supposed to influence the situation near the extraction well, so these are modeled to be far away (700 m). At the bottom of the aquifer, the salt is placed, by adding a concentration of a solute to the water in bottom layer of the aquifer. To create upconing of salt, the extraction well at the top is set to pump water outside of the system. When pumping starts, a pressure head field is created (Figure 2.2), which allows for a radial flow of water towards the well. As time passes, more and more water is extracted from every part of the aquifer. Since the water at the bottom layer of the aquifer contains a concentration of salt, this saline water is also gradually extracted, leading to a rising cone of saline water. This scenario will be modeled to determine the vertical extent of this rising salt cone, and the salt concentration of the extracted water. The **two main processes** that will be examined are (1) the effect of dispersion to the development of a mixing zone and (2) the role of density-dependent flow.

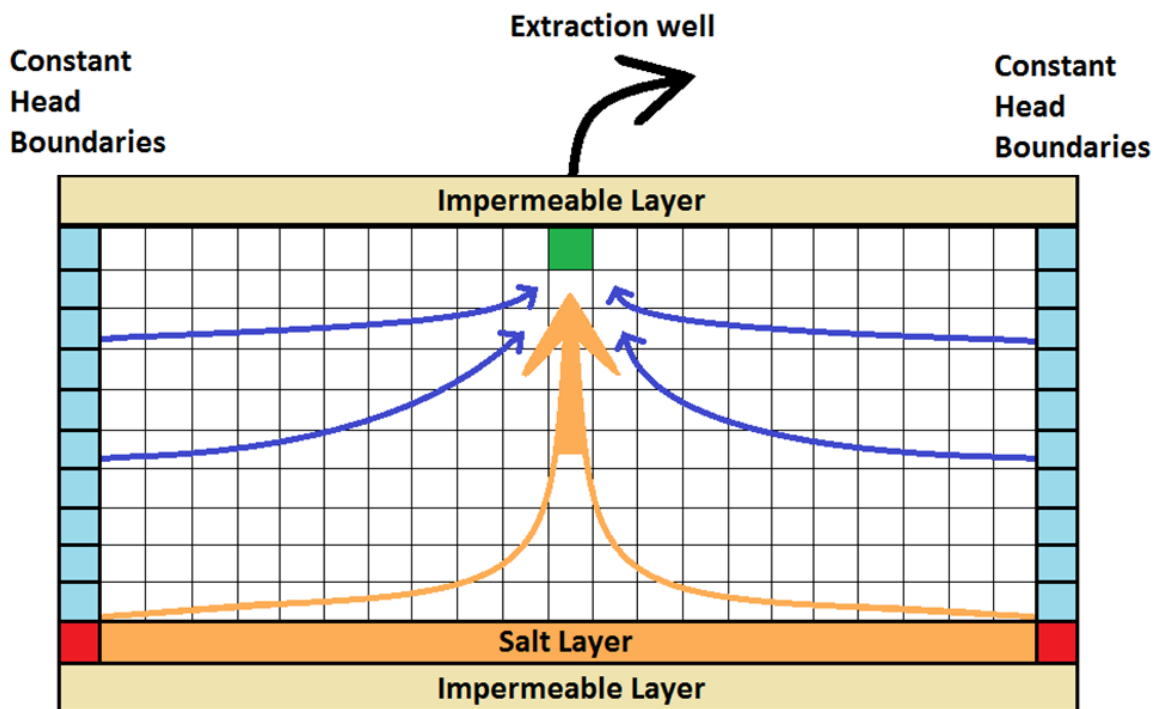


Figure 2.1: Cross-section of the conceptual model. **green:** cell with the extraction well, creating a pressure head field that generates flow towards the well. **light blue:** cells at the boundaries of the model with a constant hydraulic head value. **red:** cells at the boundaries of the bottom layer of the model that have a constant head value and a constant concentration value. **orange:** flow arrows of saline water towards the well. **dark blue:** flow arrows of the water from the constant head boundaries towards the well.

2.2 Modelling methods

To model this scenario, we use Groundwater Vistas Version 7.19 (Rumbaugh & Rumbaugh, 2017). This program uses the MODFLOW code (McDonald and Harbaugh, 1988; Harbaugh et al., 2000) and contains the necessary MT3DMS and SEAWAT2000 v4 extension (Langevin et al., 2008; Zheng & Wang., 1999). The model is considered as a three-dimensional grid of a confined aquifer, surrounded by fixed boundary conditions on all sides (except the top and bottom side). These boundary conditions are set to a constant head value (10 m) for every layer except the bottom layer. This layer is set to a constant head (10 m) and a constant concentration value of 35 [kg/m³]. In the center of the 3D domain at the top layer, an extraction well is placed, that creates a pressure head field. As the pumping well extracts water from the aquifer, the solute is slowly transported to the well and at a certain moment the salt is extracted from the aquifer.

Salt transport can be modeled by either the MT3DMS extension or the SEAWAT extension. The MT3DMS method treats the solute as a non-reactive tracer, without taking the density difference between fresh and salt water into account (Zheng et al., 1999). The transport solution technique used will be the standard finite difference method.

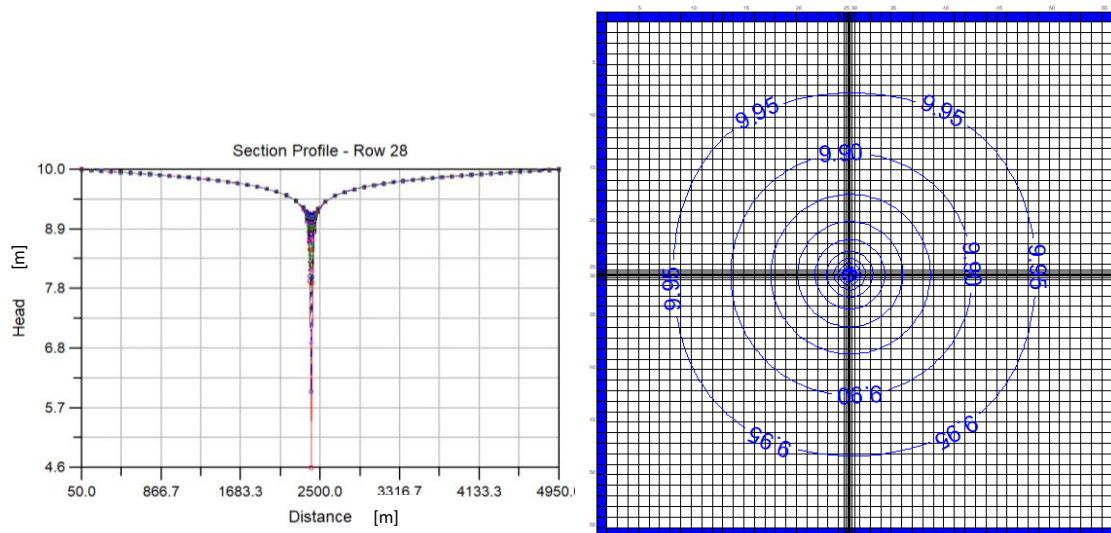


Figure 2.2: Generated pressure head field of the default scenario. **Left:** the cross-section of the pressure head, through the extraction well. **Right:** map view of the model along with the indicated pressure head contours. Values for parameters have been chosen as such that the contours were not affected by the boundary conditions, resulting in round pressure head contours.

The SEAWAT2000 version 4 code has been designed to model three-dimensional variable-density groundwater flow coupled with multi-species solute and heat transport (Langevin, C.D, 2009). The variable-density ground-water flow equation is solved using a finite- difference approximation similar to the one solved by MODFLOW-2000. The solute- transport equation is solved using one of the approaches available with MT3DMS (Langevin et al., 2008). SEAWAT2000 has been validated to specific case studies by Polemio & Romanazzi (2012), Praveena & Aris (2010) and Cai, et al. (2014).

2.3 Parameterization

2.3.1 Default scenario

Representative values for the input parameters were chosen to produce relevant model results. Studies of Powers (2007), Zuurbier (2014), and Christelis & Mantoglou (2018) were used to find relevant hydrogeological parameters for aquifers in the subsurface in western parts of the Netherlands. Table 2.1 in the following section shows each value that was chosen for the default model. All other variables were set to its default value in Groundwater Vistas Version 7.19 (Rumbaugh & Rumbaugh, 2017).

Physical parameters	Default value	Value based on
Pumping rate (Q)	400 [m ³ /day]	(Powers, 2007)
Horizontal Hydraulic conductivity (k _{x,y})	10 [m/day]	(Zuurbier, 2014)
Vertical Hydraulic conductivity (k _z)	2 [m/day]	(Zuurbier, 2014)
Aquifer Thickness (D)	40 [m]	(Zuurbier, 2014)
Initial Salt concentration (m/v)	35 [kg/m ³]	Maximum concentration of salt water in coastal aquifers: 35 [kg/m ³], (Christelis, 2018)
Salt layer thickness (S)	1,33 [m] (Bottom model layer)	Model study specified value
Effective porosity (n _e)	0,35 [-]	(Zuurbier, 2014)
Physical Horizontal Longitudinal dispersivity (α)	1 [m]	(Zuurbier, 2014)
Initial head (h ₀)	10 [m]	Model study specified value
Specific storage (S _s)	0,01 [m ⁻³]	(Zuurbier, 2014)
Specific yield (S _y)	0,25 [-]	(Zuurbier, 2014)
Bulk density (ρ _b)	1700 [kg/m ³]	(Zuurbier, 2014)

Numerical solution parameters	Default value/setting	
Pumping time (t)	180 [days]	Most dewatering operations take between 2 weeks and 4 years (Powers, 2007)
Grid area [L ²]	25x10 ⁶ [m ²] (5 [km ²])	
Grid structure	56 rows and columns, 39 layers	
Cell size (dx, dy)	12,5 – 100 [m]	
Layers thickness (dz)	0,33 – 1,33 [m]	
Solution of flow equation Modflow:		
Matrix solution technique	Finite difference method	
Solver package	PCG2	
Head change criterion	10 ⁻⁶	
Maximum Outer iterations	100	
Residual criterion for convergence	10	

Solution of tracer transport equation MT3DMS:		
Advection term	Finite difference method	
Dispersion and source terms	Implicit finite difference; generalized conjugate gradient	
Time settings	4 stress periods: 45 [days] each; 10 timesteps; 1,2 Time step multiplier	
Concentration convergence value	10^{-7}	
Solution of density-dependent transport equation SEAWAT2000 V4:		
Fluid density calculation	1- Species 1 couples flow and transport	
Minimum fluid density (ρ_{fresh})	1000 [kg/m ³]	
Maximum fluid density (ρ_{salt})	1025 [kg/m ³]	
Reference fluid density (ρ_{fresh})	1000 [kg/m ³]	
Maximum number of coupling iterations	10000	
Convergence parameter for coupling iterations	10^{-7}	
Density-concentration slope	0,71	
First time step size	0,01	

Table 2.1: All hydrogeological and numerical input parameters of the model.

2.3.2 Sensitivity Analysis: Modelling tracer transport

To assess the importance of various hydrogeological parameters for upconing of salt, a sensitivity analysis has been conducted. Multiple parameters and state variables were varied from their representative value in the default model to a range of values in order to assess the effect on salt upconing and the amount of salt that was extracted by the well. The results of this analysis will be discussed in the following section. The mass balance error margin was consulted after every run to make sure this was below 1% error. The sensitivity analysis was conducted with the MODFLOW2000 and MT3DMS code. We use MT3DMS for this analysis since its computational time is lower than that of SEAWAT2000 v4. Also, we want to have a clear view of the relationships between the parameters, without the density overcomplicating these relations.

Parameter	Default value	Ranged values
Pumping rate (Q)	400 [m ³ /day]	0 – 500 [m ³ /day]
Pumping time (t)	5000 [days]	0 -5000 [days]
Hydraulic conductivity (k _{x,y,z})	2 [m/day]	0,1 – 20 [m/day]
Aquifer Thickness (D)	40 [m]	5 – 40 [m]
Initial Salt concentration (C ₀)	35 [kg/[m ³]	1 – 300 [kg/m ³]
Salt layer thickness (S)	1,33 [m]	1 – 40 [m]
Porosity (n _e)	0,35 [-]	0,05 – 0,4 [-]
Horizontal Longitudinal dispersivity (α)	1 [m]	0 – 30 [m]

Table 2.2: parameter values used in the sensitivity analysis.

2.4 Analysis difference MT3DMS and SEAWAT2000 v4

2.4.1 New method: MT3DMS corrected

We would like to approach the results of SEAWAT2000 v4, without needing to run SEAWAT2000 v4. We can accomplish this by modifying the settings of MT3DMS as such, that the solute moves slower through the medium. This modification would lead to a salt cone that rises less, like it would do when this saline water would have been heavier. we can apply this by pretending a chemical reaction takes place between the solute and the porous medium. This chemical reaction involves adsorption of the solute particles to the soil grains. In reality, salt does not react with most soil grains, but for this analysis we will model the solute as if it would react with the soil, in order to approach the results of SEAWAT2000 v4. This new scenario will be modeled with MT3DMS, thus, these results will be called the “MT3DMS corrected” results.

The corrected settings of MT3DMS will be calculated using a linear adsorption isotherm, that relates the Retardation factor (Rf) to the sorption distribution coefficient (K_d), the raw bulk density (ρ_b) and effective porosity (n_e). This relation will be is displayed in equation 3.1

$$Rf = 1 + \frac{\rho_b}{n_e} * K_d \quad \text{Equation (2.1)}$$

The retardation factor (Rf) is the ratio of the average linear velocity of the water divided by the average linear velocity of the solute. This ratio is hard to determine since water and solute velocity is not an output parameter of the model. Thus, this ratio will be obtained empirically by fitting the results of multiple values of K_d to the results of SEAWAT2000 v4.

The best fitted value of the sorption coefficient (K_d) was at K_d = 0,0001 [m³/kg]. If we use this value in equation 2.1, we will get a retardation factor of about 1,5 [-]. This means that the solute moves at roughly 2/3 of the water velocity. It is important to realize that this value is dependent on the created model and its parameters and cannot be used to generalize a retardation of saline water transport. The results of this modeling method are shown in Figure 3.11.

To assess different model results for varying conditions, multiple scenarios were created. These scenarios were modelled with these 3 different models: the **MT3DMS model**, the **SEAWAT200 v4 model** and the **MT3DMS corrected model**. These model scenarios are displayed in table 2.3.

Exactly quantifying the amount of rise of the salt cone is quite hard, since the fresh-salt water interface is characterized by a mixing zone, instead of a sharp interface. In this study, the height of the saline water cone was defined as the highest point of the mixing zone, where the salt concentration is measurable at 2 [kg/m³]. This value was determined with the minimum amount of measurable head, which is 5 [cm], as the minimum amount of concentration a grid cell should have, to be a significant cell.





Varying parameter	Model Scenario	Pumping time [days]	Aquifer Thickness [m]	Vertical hydraulic conductivity [m/day]	Pumping rate [m ³ /day]	Dispersivity (long, trans) [m]
 Increasing pumping time	Scenario 1a	14 (2 weeks)	40	2	400	1: 0,1
	Scenario 1b	30 (1 month)	40	2	400	1: 0,1
	Scenario 1c	180 (6 months)	40	2	400	1: 0,1
	Scenario 1d	730 (2 years)	40	2	400	1: 0,1
	Scenario 1e	1825 (5 years)	40	2	400	1: 0,1
	Scenario 1f	3650 (10 years)	40	2	400	1: 0,1
 Decreasing thickness	Scenario 2a	180 (6 months)	40	2	100	1: 0,1
	Scenario 2b	180 (6 months)	32	2	100	1: 0,1
	Scenario 2c	180 (6 months)	20	2	100	1: 0,1
	Scenario 2d	180 (6 months)	12	2	100	1: 0,1
	Scenario 2e	180 (6 months)	4	2	100	1: 0,1
 Increasing conductivity	Scenario 3a	180 (6 months)	40	2	400	1: 0,1
	Scenario 3b	180 (6 months)	40	30	400	1: 0,1
 Increasing dispersivity	Scenario 4a	180 (6 months)	40	2	400	0: 0
	Scenario 4b	180 (6 months)	40	2	400	5: 0,5

Table 2.3: Scenarios to analyze the difference between the numerical models.

3 Results & Discussion

3.1 Tracer transport with MT3DMS

3.1.1 Pumping time

In this chapter, we will review the results of all models. In this first section (3.1.1), The relationship between the time you pump, and the amount of salt you will extract, is reviewed. Afterwards, the sensitivity analysis will be discussed (section 3.1.2) to determine the effect of the different input parameters. Next, the comparison between tracer transport modelling and density-dependent flow modelling will be done. Lastly, we will compare modeled results to analytical results, including the effects of dispersion to the mixing zone.

The relation between pumping time and the mass flux of salt extraction is neither entirely linear nor entirely exponential. As shown in Figure 3.1, salt extraction increases exponentially until it approaches a steady state situation. Once steady state is reached, the salt cone does not change shape anymore and can be considered to be in an equilibrium. Until this moment, groundwater and solute transport flow can be considered to be transient in time. According to study of Mercado (1969), the equilibrium is reached relatively quickly, and the salt-fresh water interface would remain to be on a certain height, independently of the pumping time. Both MT3DMS model and SEAWAT2000 v4 modelling results do not comply with this theory. Using both numerical models, salt extraction was found to keep increasing as pumping time increases. However, results of both numerical models do approach a linear trend line, as shown in Figure 3.1.

It takes a long time to approach this linear trend line. Only after $t = 5000$ days (14,8 years), this relation can be considered to become linear. However, this is probably a result of the spatial limitations of the model. It is at this time, that an equilibrium is created between the amount of salt that is extracted at the well, and the amount of salt that flows in the system at the constant concentration boundaries at the bottom layer. Thus, after 14,8 years, the model is affected by the boundary conditions, under these hydrogeological conditions. In a real world scenario, this spatial limitation does not necessarily exist, so a pure steady state salt cone would never fully develop. If the well becomes fully penetrating, the system does reach a steady state situation much faster, as visible at the left trend line in Figure 3.1. In this scenario, water flows much faster towards the well and a saline water cone is not present. As such, steady state is reached after just a few days.

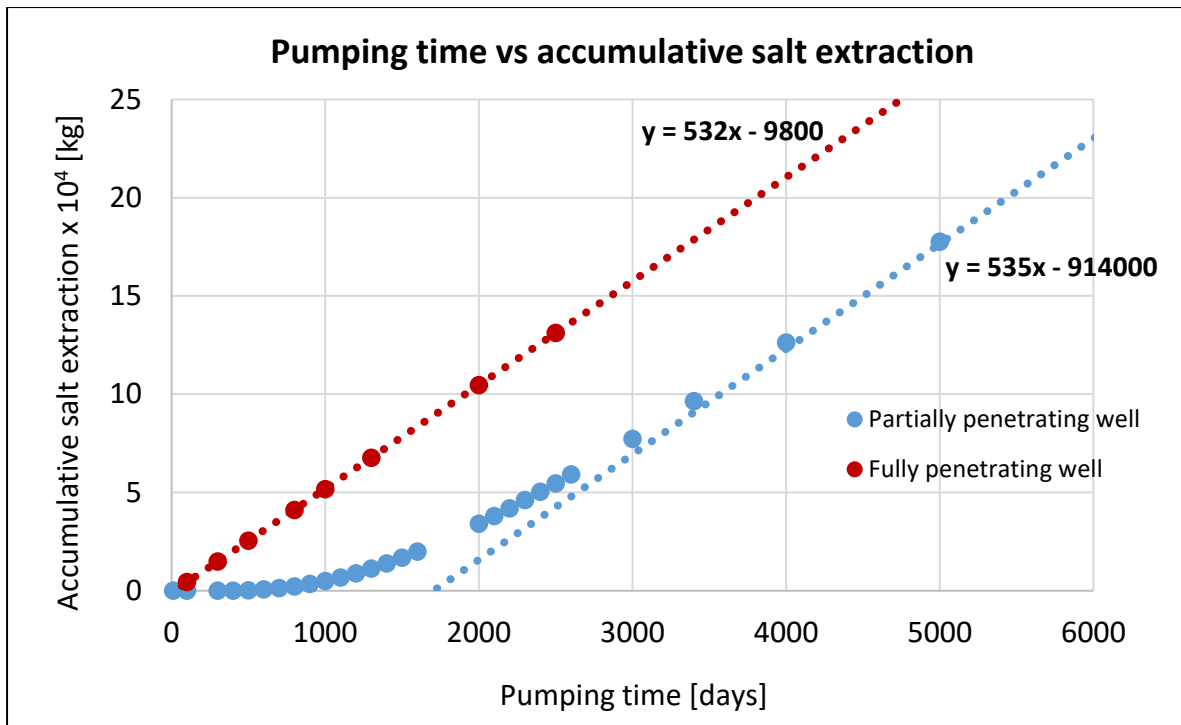


Figure 3.1: Comparing pumping time with salt extraction for 2 different scenarios. The blue symbols indicate the default scenario. It is visible that at short pumping times, salt extraction increases exponentially until a linear trend is obtained. This trend line was determined with data points at high pumping times (5000-10.000 days of pumping). The red symbols are that of the fully penetrating well. Data points display a linear relationship which is fitted with the red dotted line, at much shorter pumping times, meaning the system reaches steady state a lot sooner.

The steady-state situations of the fully penetrating well and the partially penetrating well can be displayed by linear trend lines. These linear trend lines have an almost equal slope. If we neglect the small difference in slope between both steady state scenarios, we can read from Figure 3.1, the mass flux of both scenarios: $dm/dt = 532$ [kg/day] and $dm/dt = 536$ [kg/day]. We can assume this value is fairly similar for both scenarios. This means that the mass flux (dm/dt) is equal and constant (since it is steady state). We know for a fact that for steady state the equation for non-reactive solute transport:

$$\frac{dm}{dt} = Q \cdot \bar{C} \quad \text{Equation (3.1)}$$

In this formula, \bar{C} equals the average concentration of the recovered water, and Q equals the well extraction rate. The slope in Figure 3.1 represents the ratio of mass increase per time increase, thus the first half of equation 2.1. If we use equation 2.1 to calculate the average concentration of the extracted water from the well (\bar{C}), we need to divide the slope by the pumping rate of 400 [m³/day]. From equation 2.1, we will get $\bar{C} = 1,34$ [kg/m³].

In addition, we know that during steady state salt extraction, the pumping well extracts approximately the same amount of water and concentration from each layer (Langevin et al., 2008). For this analysis a maximum concentration of 40 [kg/m³] was used (V. Christelis, 2018). Thus, if we distribute the initial concentration of 40 [kg/m³] in the bottom 1,33 meters over the remaining thickness of the aquifer, the average concentration will be the same as the initial thickness of the salt layer (Equation 3.2).

$$\bar{C} = \frac{\sum_i C_i H_i}{\sum H_i} \quad \text{Equation (3.2)}$$

This equation is a discretized average over the number of cell layers (i) representing the thickness. If we fill in this formula and divide 40 [kg/m³] over 30 [-], we will get an average concentration (\bar{C}) of 1,33 [kg/m³]. We can use this value of \bar{C} to verify that, during steady state conditions, the same amount of water is extracted from every layer, leading to an average concentration (\bar{C}), which is equal to thickness of the initial salt layer. It is interesting to see that the average concentration calculated with the model results, coincides with its theoretically calculated value. This is a verification that the model results are trustworthy. This method is dependent on the grid size of the model and cannot be used for real-world scenarios in its current form. However, if we use the non-discretized version and replace the summation operators for integration operators, we can use this for physical situations.

3.1.2 Sensitivity analysis

Pumping rate

Pumping rate was varied between 0 and 500 [m³/day]. As the pumping rate increases, more salt is extracted. However, whether this relationship is linear or exponential depends on the pumping time. If this relation is exponential, we are dealing with transient flow and if this relation is linear, we are dealing with steady state flow. A lower pumping rate requires a longer pumping time to obtain the steady state situation. Figure 3.2 shows that the longer the pumping time, the more linear the trend becomes, and the more it approaches the line $y = 1,33x$. This is the same relationship as described in equation 2.2. This can be considered to be the “ultimate steady state situation”. As pumping time increases, the more the system reaches towards this “ultimate steady state”. All other trend lines are a result of transient flow, since the mass flux is taken at a time that steady state was not reached yet. Even after 5000 days, solute flow is not fully in a steady state situation yet. In the following sections of the sensitivity analysis, when we discuss a steady situation, we refer to this situation after 5000 pumping days.

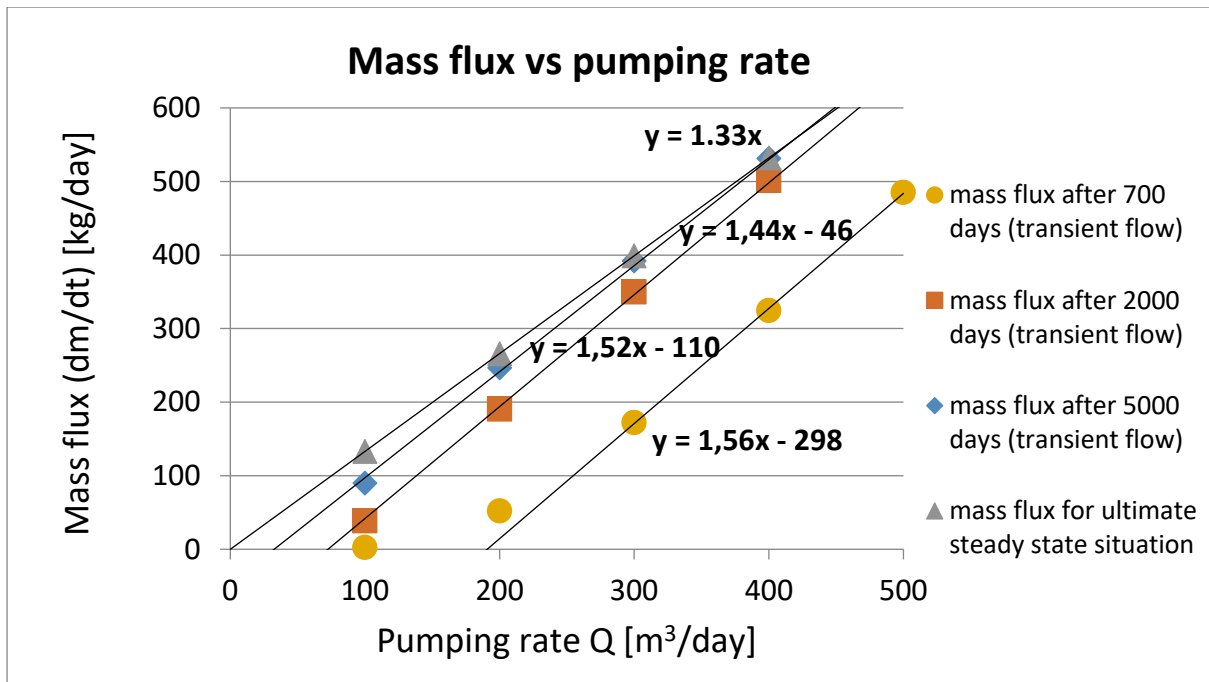


Figure 3.2: This figure shows that for longer pumping times (through mass flux after a certain amount of days), that solute flow more and more reaches to a steady state situation. The longer the stress period, the more the trend line reaches towards the ultimate steady state situation with a flux rate of 1,33 [kg/day], as calculated in the previous section. Trend lines with a different slope have not yet reached the ultimate steady state situation of 1,33 [kg/day].

Pumping rates of more than 500 [m³/day] could not be modeled because of spatial limitations of the model. Even at a pumping rate of 500 [m³/day], the cone of depression is slightly affected by the boundary conditions of the model as visible in Figure 3.3. The 5 [cm] drawdown contour is no longer a perfect circle, as it was at Q= 400 [m³/day] as visible in Figure 2.2.

Vertical Hydraulic conductivity

The vertical hydraulic conductivity (k_z) was varied between 0,1 – 20 [m/day]. It was found that the higher the conductivity, the more salt is extracted. This is logical, because water can flow easier through the aquifer, and more saline water can reach the well. This relationship, however, is **not linear** in steady state conditions. A higher hydraulic conductivity leads to exponentially more salt extraction.

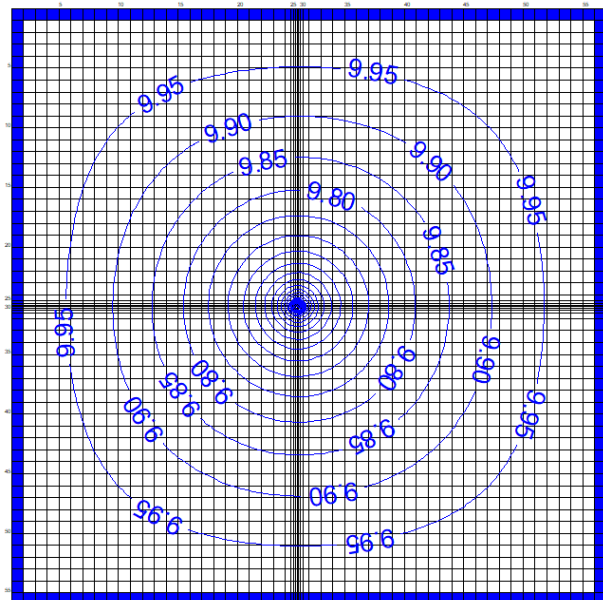


Figure 3.3: Representations of head contours of layer 1 of the model with Q= 500 [m³/day]. The 5 [cm] drawdown contour is no longer a perfect circle.

However, if we plot the rate of salt extraction after six months (180 days), versus vertical hydraulic conductivity, we see a linear trend emerging (Figure 3.4). The rate of salt extraction (mass flux) increases linearly as the conductivity increases, but there is a certain threshold value for the conductivity to start salt extraction. This is reached when the linear trend line crosses the x-axis at the value of $k_z = 4,1$ [m/day]. This can be considered to be the minimum conductivity for salt extraction to occur, in these conditions. If we want to apply this analysis for specific field studies, we should apply this to our the more advanced model SEAWAT2000 v4. If we conduct the same analysis with SEAWAT2000 v4, the minimum value of k_z will be 5,9 [m/day]. However, it is important to realize that these minimum values of the hydraulic conductivity are not constant. They are still dependent on other hydrogeological factors and the pumping rate. If we apply a higher pumping rate, this minimum value of the conductivity will be lower.

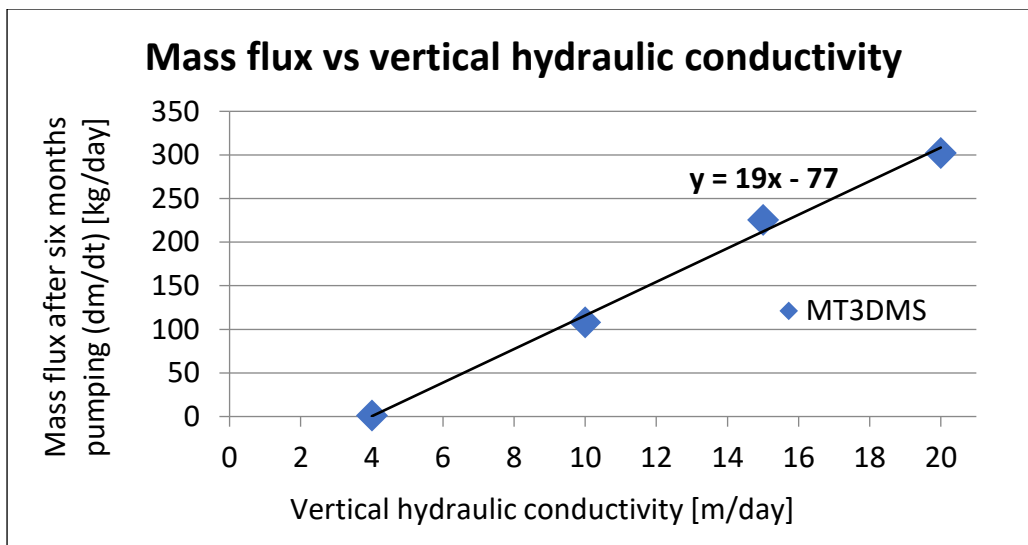


Figure 3.4: Mass flux vs vertical horizontal conductivity at the stress period time difference of $t = 180$ [days] and $t = 190$ [days] The intersection of the trend line with x-axis occurs at $x = 4,1$. Thus, we can conclude that the minimum value of k_z for salt extraction to occur is at 4,1 [m/day] for MT3DMS.

Thickness of salt layers

It was found that the number of salty layers **linearly** relates to the mass of salt extraction (Figure 3.5). As such, every single layer contributes for the same amount of salt that is being extracted, during steady state conditions. This relation is also shown in equation 2.3. Figure 3.6 shows multiple cross-sections for different amounts of salty layers. If we vary pumping rate Q , the linear relationship still holds. One salty layer has a thickness of 1,33 [m].

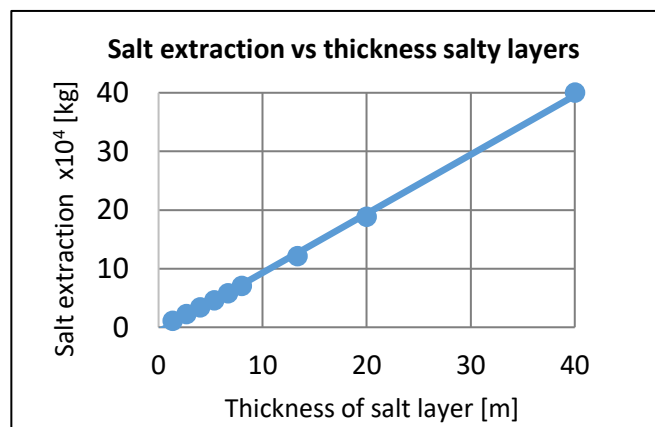


Figure 3.5: Salt extraction vs thickness of salty layers. In steady state conditions, every layer contributes for the same amount of salt uptake from the extraction well.

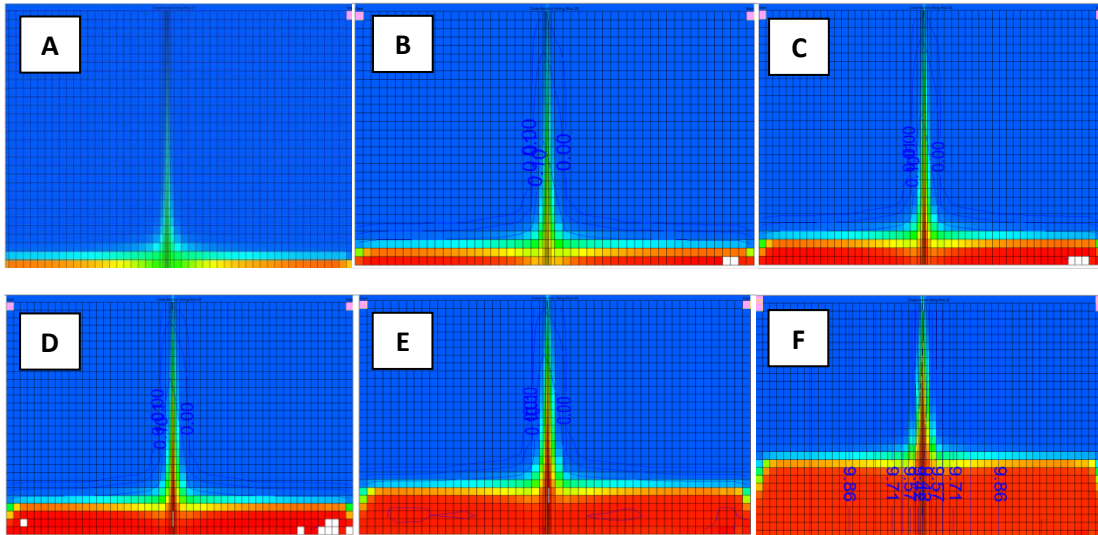


Figure 3.6: Six different cross-sections of the model, displaying different amounts of salty layers in the default model. (A): 1 salty layer, (B): 2 salty layers, (C): 3 salty layers, (D): 4 salty layers, (E): 6 salty layers, (F): 9 salty layers.

Aquifer thickness

The acquired relationship between salt extraction and the thickness of the aquifer is also non-linear. Thinner aquifers lead to exponentially more salt extraction, as visible in Figure 3.7. This parameter had to be examined using a smaller extraction rate of 100 [m³/day]. The default parameter of 400 [m³/day] caused the 5 [cm] drawdown circle to become non-circular at shallow aquifer depths. Thus, the relationship could only be defined at lower pumping rates. Figure 3.7 shows that only at aquifer thicknesses lower than 20 meters, the concentration becomes significant. The right graph of Figure 3.7 shows that if the ratio becomes larger than 0,05 (1 salt layer for 20 total layers), concentration increases linearly. This shows that under these hydrogeological conditions, a thickness of 20 meters can be considered a threshold value. It is important to realize that this value is still dependent on other variables, like the pumping rate. The thickness of the aquifer can be considered an important variable, since it determines the vertical distance of the saline water to the extraction well.

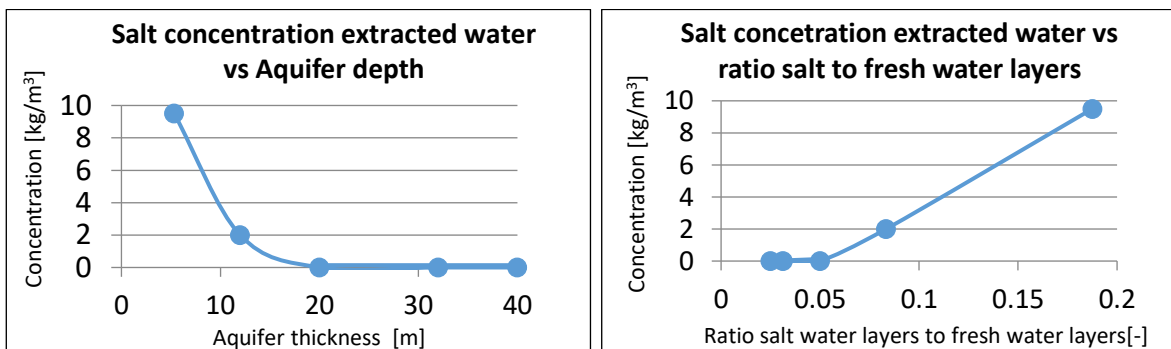


Figure 3.7: **left:** Concentration of extracted water versus aquifer depth. Only at aquifer thicknesses lower than 20 meters, the concentration becomes significant. **right:** concentration of extracted water vs ratio of salt water layers vs fresh water layers. If the ratio becomes larger than 0,05 (1 salt layer for 20 total layers), concentration increases linearly with the ratio.

Dispersion

The dispersion is the driving mechanism that creates the mixing zone between the salt-fresh water interface. Variations of pore velocity of the solute flow lead to the creation of preferential flow paths of the solute (van Ommen, 1990; Landman et al., 2007; Egorov et al., 2005). This causes some particles to move faster towards the extraction well and some particles to move slower. This phenomenon can lead to a profound mixing zone. Since this dispersion is the effect of both physical and numerical dispersivity, both values have been quantified in this report

This analysis regards the effects of the **physical** longitudinal dispersivity. The numerical dispersivity cannot be varied, since this is model-inherent. The quantification of the numerical dispersivity will be shown in the appendix and was found to be: $\alpha = 2,3$ [m] .

It was found that the higher the longitudinal dispersivity, the more salt is extracted from the extraction well, and the higher the salt cone reaches. The transverse dispersivity was remained zero for this analysis. If we run this analysis for a (close to) steady state salt cone ($t = 5000$ days), we will acquire a **linear** relationship between dispersivity and salt extraction. However, if we investigate this relationship at shorter time periods, we observe a **non-linear** trend. If we plot the results of this calculation the same way as Figure 3.1, we can create Figure 3.8. We can see clearly that the higher the dispersivity, the more salt is extracted, and the easier saline water flows towards the well.

The steady state situation is reached when the data points can be represented correctly by a linear trend line. We have plotted 2 other scenarios: one scenario with increased physical dispersivity: $\alpha = 5$ [m], which are represented by the purple data points, and one scenario where physical dispersivity was set to zero: $\alpha = 0$ [m], represented by the green data points. The total dispersivity values are the physical dispersivity combined with the numerical dispersivity values. These values are shown in Figure 3.8. We can also conclude that the higher the dispersivity, the sooner a steady state situation is reached.

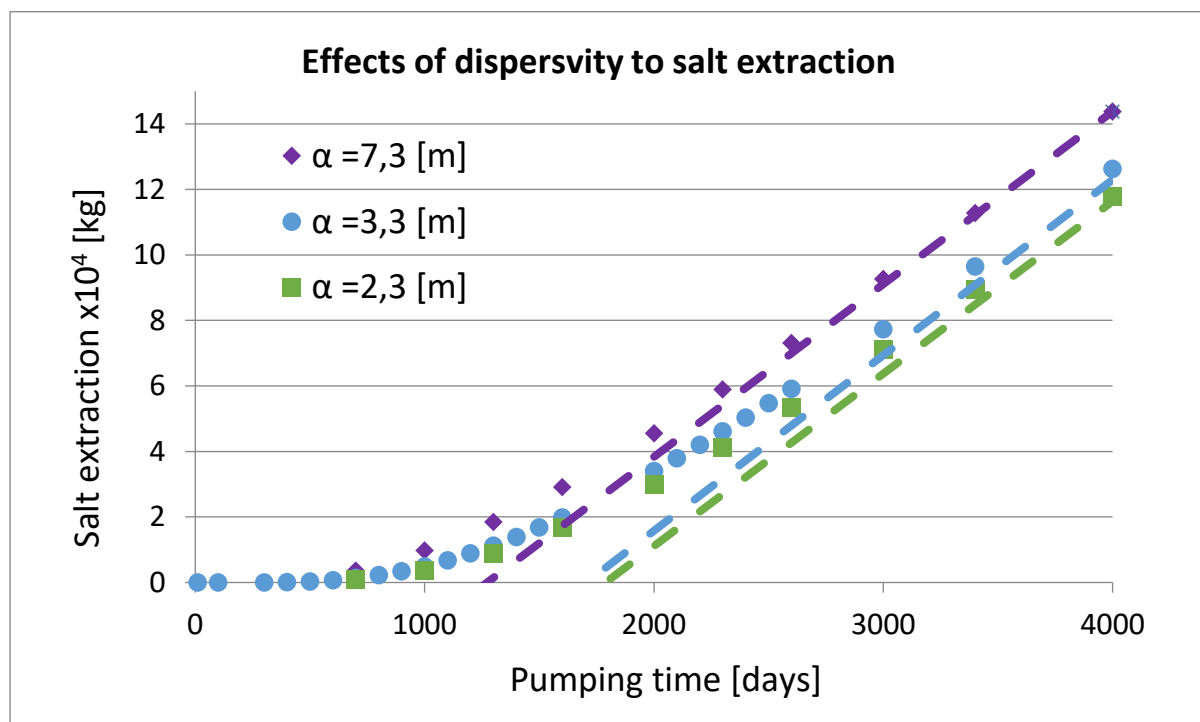


Figure 3.8: Salt extraction vs pumping time, varying dispersivity. The dotted line represents the steady state trend line for each scenario. The higher the dispersivity, the sooner the system reaches steady state, and the more a mixing zone develops.

Porosity & Initial concentration

The other two varied parameters both had a **linear** relation with salt extraction, in steady state conditions. It was found that the higher the initial concentration, the more salt is extracted from the extraction well (Figure 3.9).

Porosity had a negative correlation to the amount of salt extraction: the higher the porosity, the less salt is extracted. This can be explained by the fact that a smaller the pore size, leads to a higher pore velocity. Thus, a lower porosity leads to more solute transport towards the well, at a constant hydraulic conductivity. Hydraulic head, specific yield and specific storage had no effect on result outcomes. The plots are jointly presented in Figure 3.9.

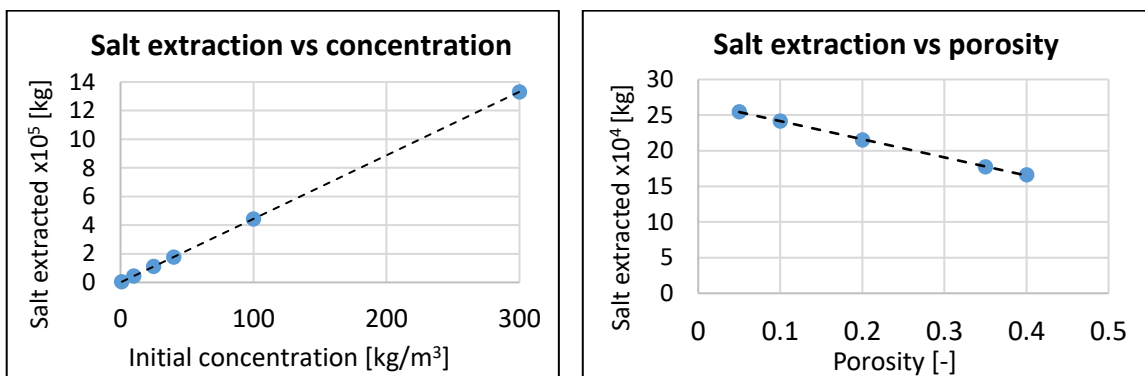


Figure 3.9: left: Salt extraction versus initial concentration after 5000 days of pumping. **Right:** Salt extraction versus porosity. All show a linear trend during steady state conditions after 5000 days of pumping.

3.2 Tracer transport vs density-dependent flow

3.2.1 General Results

In this section we will discuss the results of the scenarios that compared the displayed with 3 different models: the **MT3DMS model**, the **SEAWAT200 v4 model** and the **MT3DMS corrected model**. Model results will be discussed based on 2 main criterions: Salt concentration of extracted water and the vertical rise of the saline water cone. The results are displayed in table 3.1 and visualized in Figure 3.10. Inflow from the constant concentration boundaries at the bottom layer were found to be zero for every scenario.

Model Scenario	MT3DMS		SEAWAT2000 v4		MT3DMS corrected	
	Result: Rise of top of mixing zone [m]	Result: Salt concentration of the extracted water [kg/m ³]	Result: Rise of top of mixing zone [m]	Result: Salt concentration of the extracted water [kg/m ³]	Result: Rise of top of mixing zone [m]	Result: Salt concentration of the extracted water [kg/m ³]
Scenario 1a	0,05	0	0,05	0	0,05	0
Scenario 1b	0,1	0	0,1	0	0,3	0
Scenario 1c	5,10	0	2,7	0	2,4	0
Scenario 1d	24,00	0,03	10,7	0,003	13,3	0,012
Scenario 1e	33,40	0,33	26,8	0,008	31,3	0,11
Scenario 1f	36,1	0,71	32,0	0,31	34,7	0,42
Scenario 2a	0,15	0	0,15	0	1	0
Scenario 2b	1,40	0	1,20	0	1,7	0
Scenario 2c	6,70	0	4,7	0,003	6	0,46
Scenario 2d	12 (max)	2,00	12 (max)	0,87	12 (max)	1,2
Scenario 2e	5,33 (max)	9,50	5,33 (max)	5,95	5,333 (max)	8,0
Scenario 3a	5,10	0	2,7	0	2,4	0
Scenario 3b	25,4	0,63	22,7	0,31	25,3	0,34
Scenario 4a	2,0	0	2,0	0	1	0
Scenario 4b	27,7	0	26,7	0	25,3	0

Table 3.1: Results tracer transport vs density-dependent flow and corrected tracer transport.

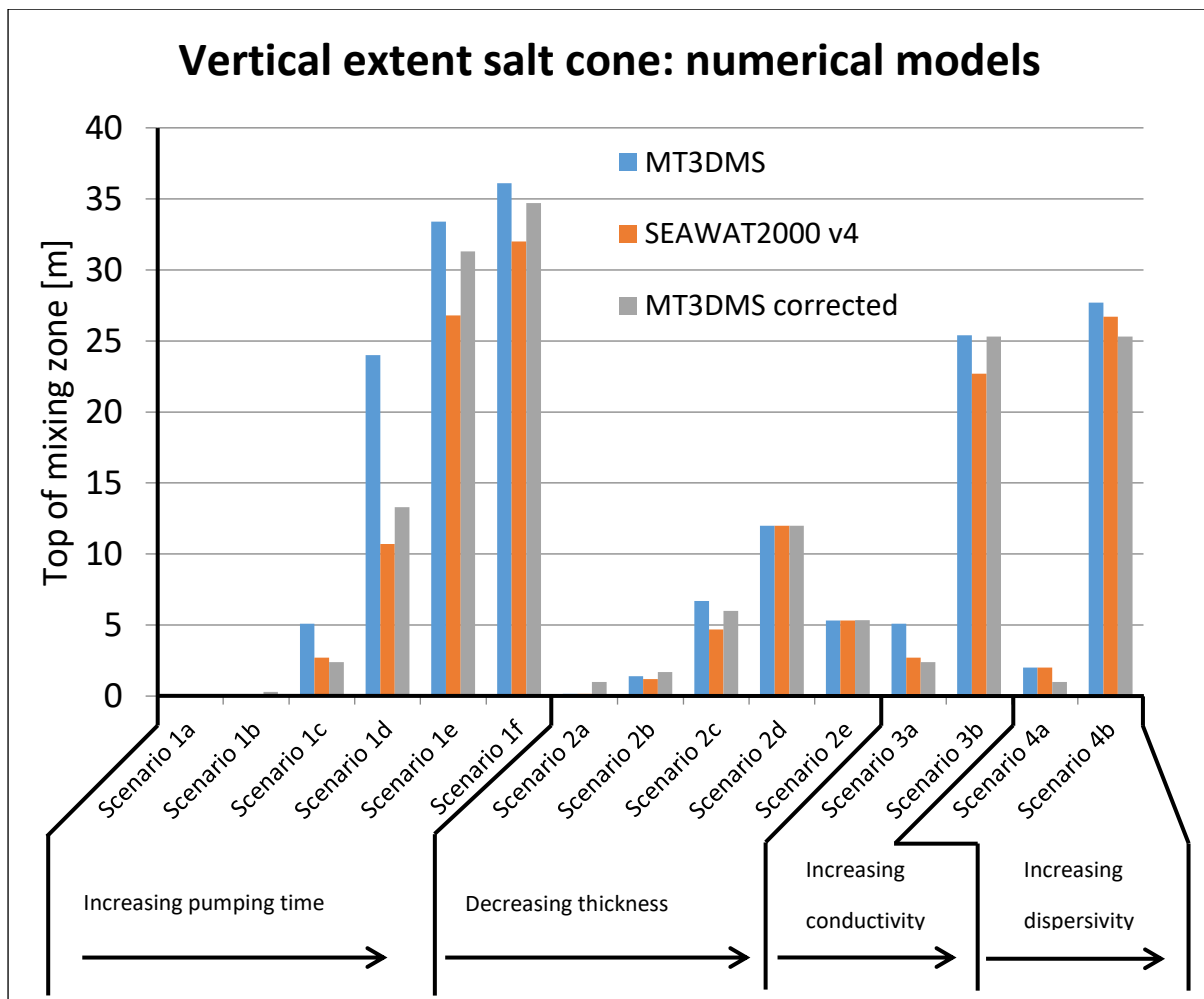


Figure 3.10: Visualization of the results of table 3.1 for the rise of the salt-fresh water interface.

3.2.3 Vertical extent of the salt cone

Figure 3.10 shows the different results of the three different numerical models. These are the results of the amount of rise of the top of the mixing zone, where concentration reaches a significant concentration of 2 [kg/m³]. It is clear that the model MT3DMS produces highest results. This makes sense, since this method models the solute as a tracer. Thus, it does not consider the extra weight of the heavier saline water. This results in more optimistic results for MT3DMS. The SEAWAT2000 v4 model is the most advanced model, so these results should resemble the most physical situation. SEAWAT2000 has been validated to specific case studies by Polemio & Romanazzi (2012), Praveena & Aris (2010) and Cai, et al. (2014). The results of MT3DMS corrected mostly lie between the results of the other two models. This is visualized more specifically in Figure 3.11.

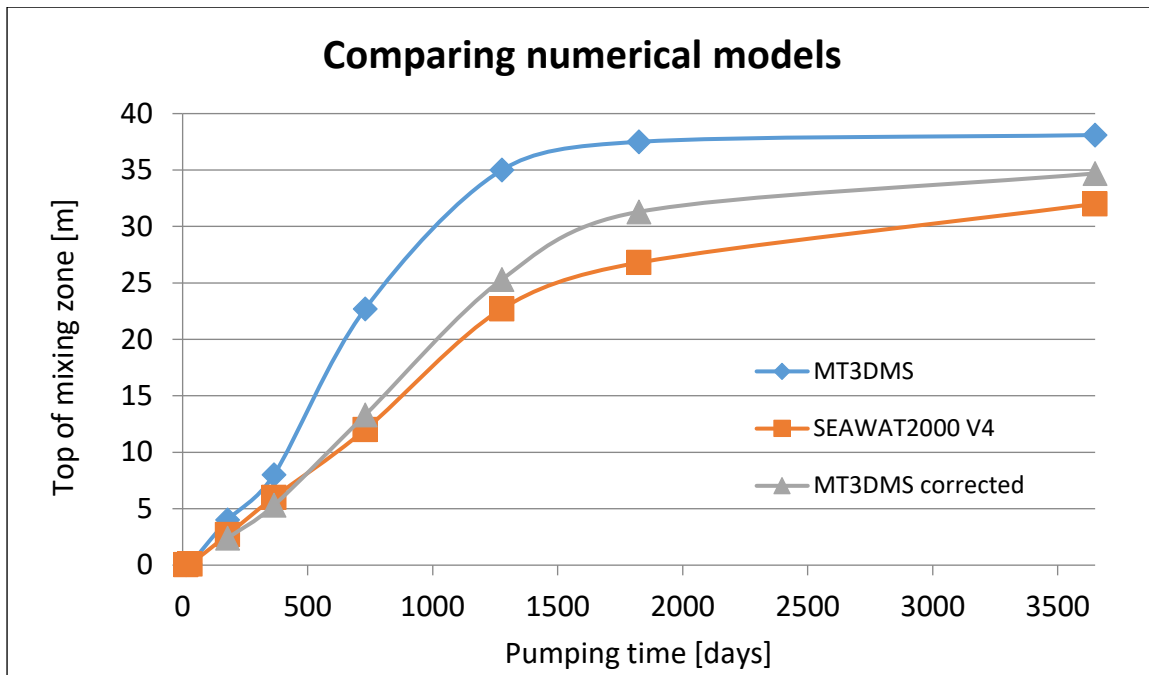


Figure 3.11: Results of the 3 different numerical models of the rise of the top of the mixing zone compared to pumping time (scenario 1a-1f).

As shown in Figure 3.11, it is possible to fit the results of MT3DMS corrected to the results of SEAWAT2000 v4. However, there are a few anomalies. As pumping time increases, the results of corrected MT3DMS and SEAWAT2000 v4 diverge, leading to an overestimation of upconing of the corrected MT3DMS scenarios. To create a curve that will fit at larger pumping times to the results of SEAWAT2000 v4, we need to use a different value for the sorption coefficient. We can fit the results for long pumping times better when increasing the sorption coefficient value to $K_d = 0,0002 \text{ [m}^3/\text{kg}]$.

Another difference between the corrected MT3DMS and SEAWAT2000 v4 results is visible during the first five years of pumping. At short pumping times (shorter than 500 days), the corrected MT3DMS results slightly **underestimate** upconing compared to the SEAWAT2000 v4 results. At longer pumping times (longer than 500 days), the corrected MT3DMS results slightly **overestimate** upconing compared to the SEAWAT2000 v4 results. In general, results of SEAWAT2000 v4 are more linear and results of MT3DMS are more affected by limiting boundary conditions on the bottom and the top of the aquifer. This might be the result of the more viscous behavior of saline water, when modelled by SEAWAT2000 v4. However, a definite explanation for this has not yet been found.

For most cases, when pumping time is shorter than 5 years, we can state that the results of the corrected MT3DMS method match the results of SEAWAT2000 v4 well enough to be considered a valid alternative approach. Using this approach, a user could use the computationally lighter model of MT3DMS to predict salt upconing inside an aquifer, saving computational time compared to SEAWAT2000 v4. However, it is advised that the user runs the SEAWAT2000 v4 model at least once, to find the best fitting value of the sorption coefficient.

To visualize the effect of the thickness of the aquifer on the height of the top of the mixing zone, Figure 3.12 was created. The MT3DMS model again produces highest results. But the difference is not as profound. We can conclude that the thinner the aquifer, the less the difference between the models develops. Also, the thinner the aquifer, the sooner the top of the mixing zone reaches the top of the aquifer.

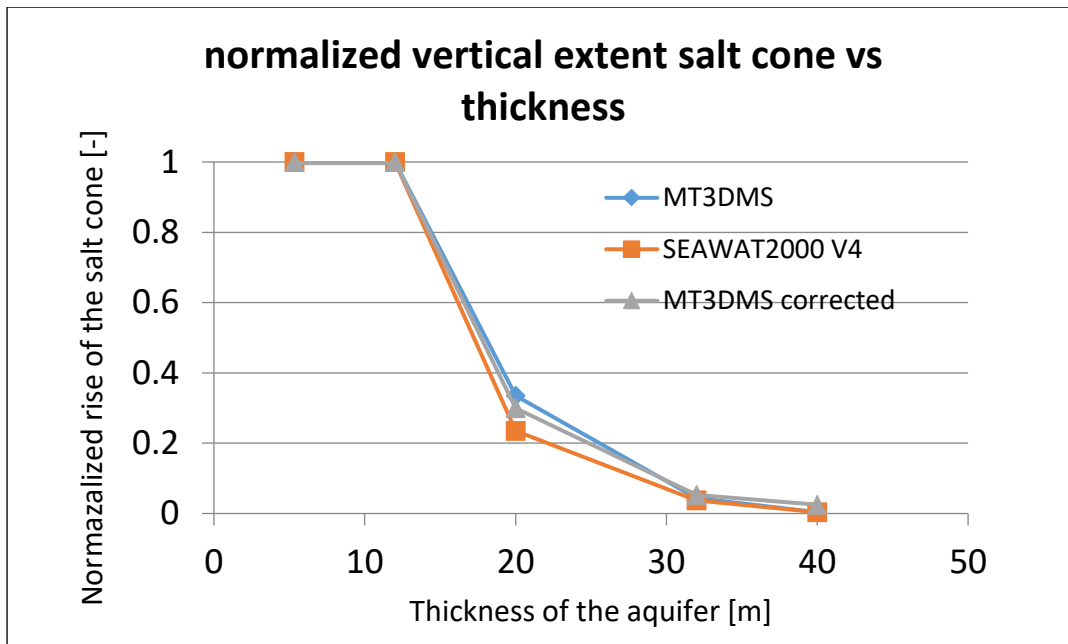


Figure 3.12: Normalized vertical extent salt cone vs aquifer thickness. The value on the y-axis represents the maximum water rise divided over the thickness. If the value on the y-axis reaches 1, the top of the salt cone has reached the top of the well. If an aquifer is less thick than 40 [m], upconing can reach the surface much sooner. If the thickness is equal or smaller than 12 [m] and the pumping rate is 100 [m³/day] for 6 months, the upconing reaches the surface.

3.2.4 Concentration of the recovered water

The extraction well extracts water from all parts of the aquifer. Thus, the salt concentration of the extracted water is strongly diluted. Even after 10 years of pumping (scenario 1f), the average salt concentration of the recovered water (\bar{C}) is only 0,31 [kg/m³], when modeled with SEAWAT2000 v4. This is below the steady-state salt concentration of 1,33 [kg/m³], calculated in section 3.1.1. This can be explained by the long duration of transient flow conditions. During transient flow, substantially more fresh water is extracted than saline water. This affects the average concentration significantly. Even when a situation is reached that is very close to steady state conditions, the total salt concentration of the recovered water (\bar{C}) is still lower than 1,33 [kg/m³]. Figure 3.13 shows the relation of the top of the mixing zone to pumping time and aquifer thickness.

Note that, during transient flow conditions, the total salt concentration (\bar{C}) is different than the concentration of saline water extracted by the extraction well at a certain moment in time. The concentration at a certain time at the extraction well can be a lot higher than the average recovered salt concentration (\bar{C}). This is the case when in first stages of pumping, there is no saline water extraction yet. During longer pumping times, salt concentrations at the extraction well can be high, while the average salt concentration (\bar{C}) is still low.

Be aware that even when the top of the mixing zone has not yet reached the extraction well, salt can already be extracted by the well, but heavily diluted. This is due to the determined significant concentration of 2 [kg/m³] of salt that the water should reach to be part of the salt cone. Thus, water with lower concentrations than 2 [kg/m³] is able to reach the well. However, this does not mean the top

of our defined mixing zone has reached the well. In physical situations, this probably also occurs, since this mixing zone is not separated with fresh water with a sharp interface

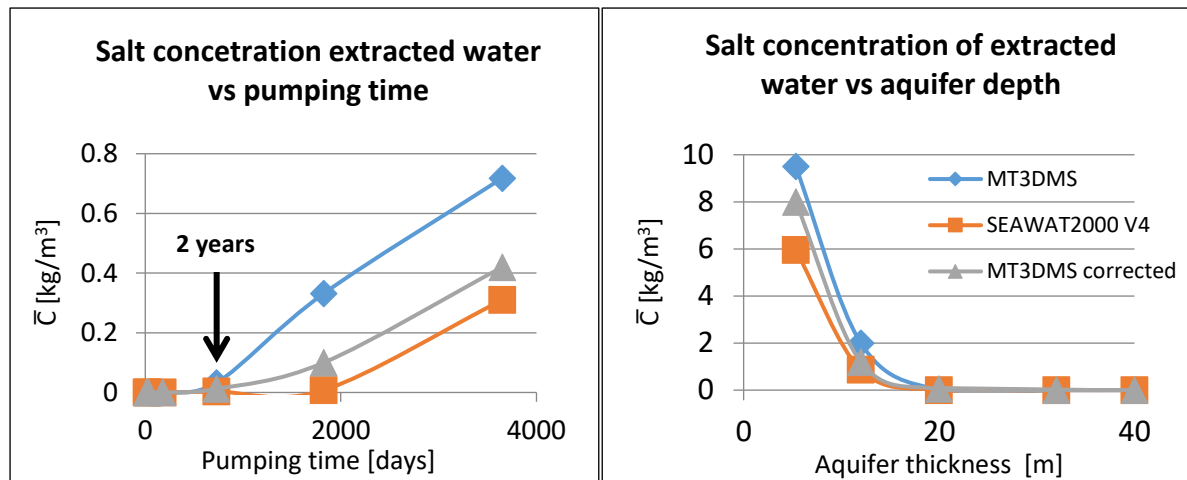


Figure 3.13: *Left:* Salt concentration of recovered water (\bar{C}) vs pumping time. Only at pumping times more than 2 years, concentration of the extracted water increases significantly. This value remains only a small fraction of the 35 [kg/m³] at the initial salt-fresh water interface. Pumping times on the x-axis are long, since the average concentration \bar{C} remains very low during transient flow conditions. *Right:* Salt concentration of recovered water (\bar{C}) vs aquifer thickness. Results of SEAWAT are more conservative than that of MT3DMS. At thicknesses thicker than 20 meters, no effect on the concentration of the extracted water is expected (for 6 months pumping time).

3.2.5 Effect of salt availability on upconing

Development of the salt cone is limited by the amount of available salt. The default conceptual model considers 1 salt layer with an inflow of saline water from the constant concentration boundary conditions on the sides. This is the appropriate model for a scenario with one salty layer on top of a consolidate layer like clay. However, for scenarios without a consolidating layer, the available salt may not be limiting the development of the salt cone. In these scenarios, the shape of the cone is mostly governed by the pumping rate and aquifer thickness. If we compare this setup with a setup with an unlimited amount of salt available, there is a large difference. Figure 3.14 shows the difference in salt cone development between the default model and a model with an unlimited amount of salt available. It is clear to see that both the width and the height of the cone is a lot more well-developed in the scenarios with an unlimited amount of available salt. Comparing both SEAWAT scenarios: the model with an unlimited amount of salt extracted 3920 [kg] of salt, while the model with 1 layer of salt atop a consolidating layer extracted only 2,5 [kg] of salt, in a period of five years. Since this difference is extremely large, it is vital to take the available salt into consideration when applying the model.

Also, it is useful to take into consideration that the interface between the fresh and saline water could be mixed already. A transition zone of 0 [kg/m³] until 35 [kg/m³] could exist in the order of centimeters to meters (Diersch et al., 1983). This transition zone is not implemented in the default model. However, we can distribute a salt concentration profile linearly at the bottom layers of the aquifer. If we run the default model with a thick mixing zone (bottom 20 meters linearly distributed from 0 [kg/m³] to 35 [kg/m³]), the salt cone is affected. The salt cone in this scenario reaches a height of 13,3 meters, instead of 2,7 meters, modeled with SEAWAT2000 v4. This difference seems large, but we need to take into

consideration that this mixing zone also results in a much shorter distance of saline water to the extraction well.

Since the salt availability is this important, it is essential to use a representative concentration-depth profile. During field-studies, this could be acquired by a multi-depth sampler that determines the salt concentration at varying depths.

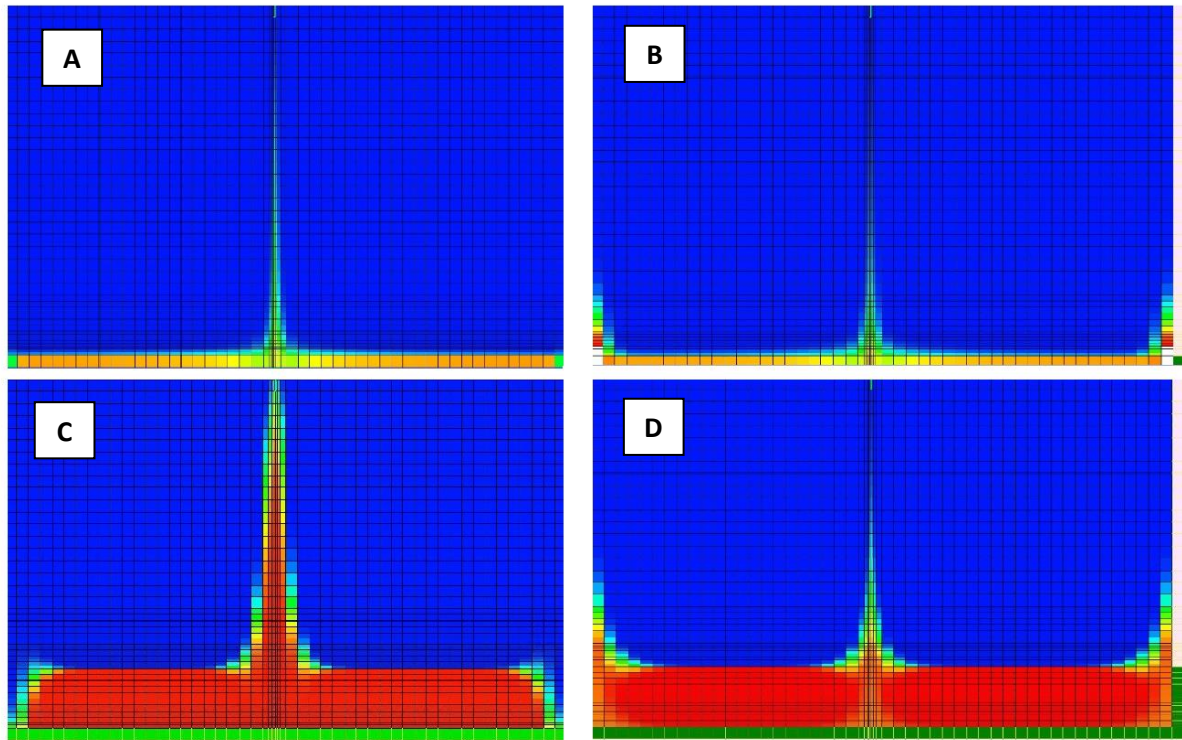


Figure 3.14: 4 different scenarios for salt cone development inside the default model. **A:** 1 salt layer (1,33 m) model solved with MT3DMS. **B:** 1 salt layer (1,33 m) model solved with SEAWAT V4. **C:** 8 salt layers (12 m) model solved with MT3DMS. **D:** 8 salt layers (12 m) model solved with SEAWAT V4. Corresponding salt extraction calculated by the model was: **A:** 198.487 [kg] **B:** 2,5 [kg] **C:** 9.072.844 [kg] **D:** 3920 [kg].

Figure 3.14 also illustrates that an anomaly occurs near the boundary conditions of the system. Concentrations either peek downward or upward near the constant head and constant concentration boundaries. This is caused by the option to correct boundary heads for density. If this option is used, there will be a head decrease near the edges of the system, which leads to a rise of concentration. Consequently, when this option is not used, the heads will increase near the edges, causing a decrease of concentration. There was no method that did not cause any anomalies at the edges of the system. However, if we compare the effect of both anomalies on the amount of salt extraction by the pumping well, there is no difference in both scenarios. Both modeled results showed no consequence on the amount of extracted salt. In other words, the inflow of saline water from the boundary conditions inside the system does not have a significant effect on salt extraction in the center of the system, meaning most extraction occurs locally.

3.3 Comparison of numerical models to analytical solutions

3.3.1 Radial flow equation

The analytical solution for radial flow to a well in a confined aquifer can be directly derived from combining Darcy's flow equation and the mass balance equation (Fitts, 2002). The derivation can be found in the book Groundwater Science by Fitts (chapter 6.2). Equation 3.3 displays the radial flow equation to a well.

$$h_1 - h_0 = \frac{Q}{2\pi kD} \ln\left(\frac{r}{r_0}\right) \quad \text{Equation (3.3)}$$

In this formula, radial distance to the extraction well is represented by (r) and radius of the extraction well is represented by (r_0). The generated pressure head field in the default scenario created a drawdown (h_1-h_0) of 2 [m]. At a radial distance of 1820 [m], the pressure had was at the same value as the initial head (h_0), during steady state flow. The well radius (r_0) was set to 0,1 [m]. The equation does have a few assumptions: (1) water flow is steady state, (2) resistance to vertical flow is neglected, (3) the aquifer thickness and hydraulic conductivity is homogeneous and constant and (4) the well is fully penetrating.

Combining equation 3.3 with equation for non-reactive solute transport (equation 3.1) will lead to the following equation:

$$\frac{dm}{dt} = \bar{C} * Q = \frac{\bar{C} * 2\pi kD * (h_1 - h_0)}{\ln\left(\frac{r}{r_0}\right)} \quad \text{Equation (3.4)}$$

Solving this equation for the default scenario, leads to a theoretical mass flux that we can compare to the mass fluxes of the numerical models, while varying vertical hydraulic conductivity (Figure 3.15).

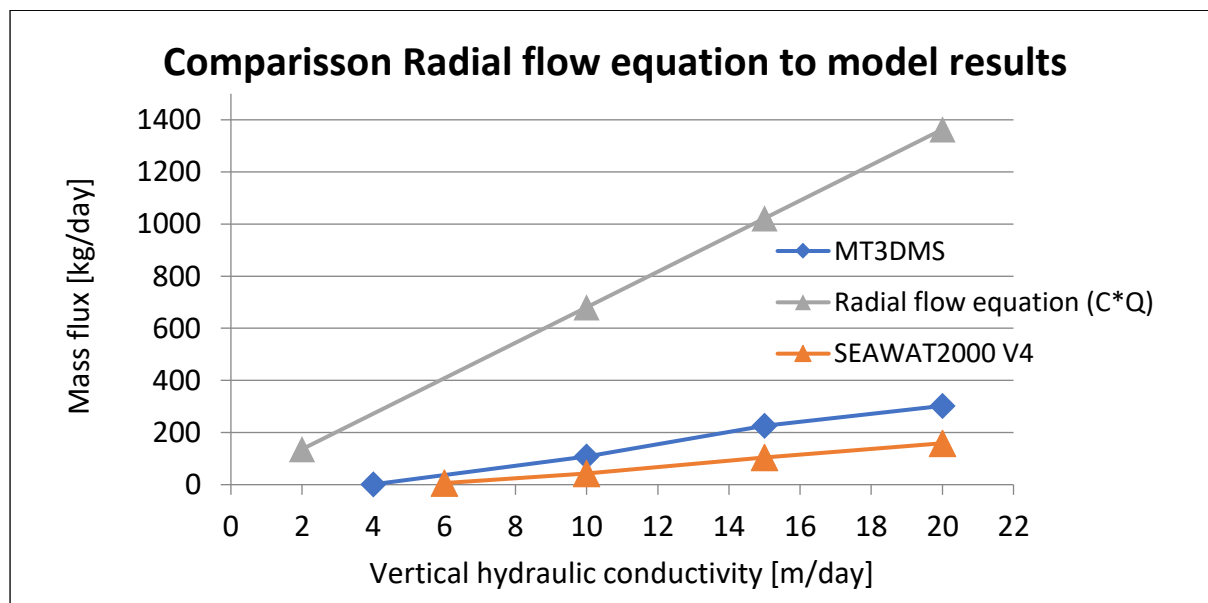


Figure 3.15: Mass flux vs vertical horizontal conductivity at the stress period time difference of $t=180$ [days] and $t=190$ [days]. The theoretical extraction rate (mass flux) is shown in **gray** (equation 3.4), compared to the modeled result of the mass flux in **blue** for MT3DMS and **orange** for SEAWAT2000 v4. The intersection of the trend line with x- axis occurs at $x=4,1$ for MT3DMS, and at $x=5,9$ for SEAWAT2000 v4. Thus, we can conclude that the minimum value of k_z for salt extraction to occur is at 4,1 [m/day] for MT3DMS and at 5,9 [m/day] for SEAWAT2000 v4.

The analytical solution of the radial flow equation shows a similar trend to the numerically modeled solutions. However, the analytical solutions are roughly four times higher. This can be explained through the assumptions and complications of the radial flow equation. Since the analytical solution does not consider the extra vertical resistance, due to the fact that the radial flow equation assumes the use of a **fully penetrating well**. This means the radial flow equation calculates the mass flux to be much higher. Another weakness of this method lies in the effect of the vertical hydraulic conductivity to the drawdown. A higher conductivity leads to less drawdown at the well. All these complications and assumptions make this method unsuitable as a correct analytical model verification.

3.3.2 Analytical solution of Mercado (1969)

The study of J. Wagner & D. Kent (1985) provides an analytical solution for the amount of upconing below a pumping well, based on the equations of Mercado (1969). This formula is able to determine the position of the interface and the salinity of the extracted water for a specified pumping rate. A few basic assumptions underlie the theoretical development of this cone, which are: (1) the porous medium is homogeneous and non-deformable, (2) the two fluids are incompressible, immiscible and separated by an abrupt interface, (3) the flow conforms to Darcy's law. In this equation, the vertical distance from the initial interface is represented by (X). Wagner & Kent (1985) define a slow and gradual upconing of the interface, until a certain critical rise (X_{cr}) is reached. From this distance upward, a sudden rise would lead the interface to the well. The following equations are provided to describe this phenomenon (J. Wagner & D. Kent, 1985).

$$\bar{X} = X(r, t) = \frac{Q}{2\pi\left(\frac{\Delta\rho}{\rho}\right)k_x D} * \left(\frac{1}{\sqrt{1+R^2}} - \frac{1}{\sqrt{(1+\tau)^2+R^2}} \right) \quad \text{Equation (3.5)}$$

Where:

$$R = \frac{r}{D} * \sqrt{\frac{k_z}{k_x}} \quad \text{and} \quad \tau = \frac{\left(\frac{\Delta\rho}{\rho}\right)k_z}{2n_e D} * t$$

Usually, this method is used for the vertical rise of the abrupt salt-fresh water interface. Thus, to use this method for a situation **with** a mixing zone, we need to adjust the value of the density ratio: $\frac{\Delta\rho}{\rho}$, to mimic a situation where a mixing zone is present. Instead of a density ratio of $\frac{\Delta\rho}{\rho} = \frac{25}{1000}$, we can vary this ratio from $\frac{\Delta\rho}{\rho} = \frac{25}{1000}$ to $\frac{\Delta\rho}{\rho} = \frac{2}{1000}$, for this is the determined significant concentration of 2 [kg/m³] that the water should reach to be part of the salt cone. If we plot the results of this analysis, we can create a contour plot of the salt cone. This is shown in Figure 3.16 and 3.17.

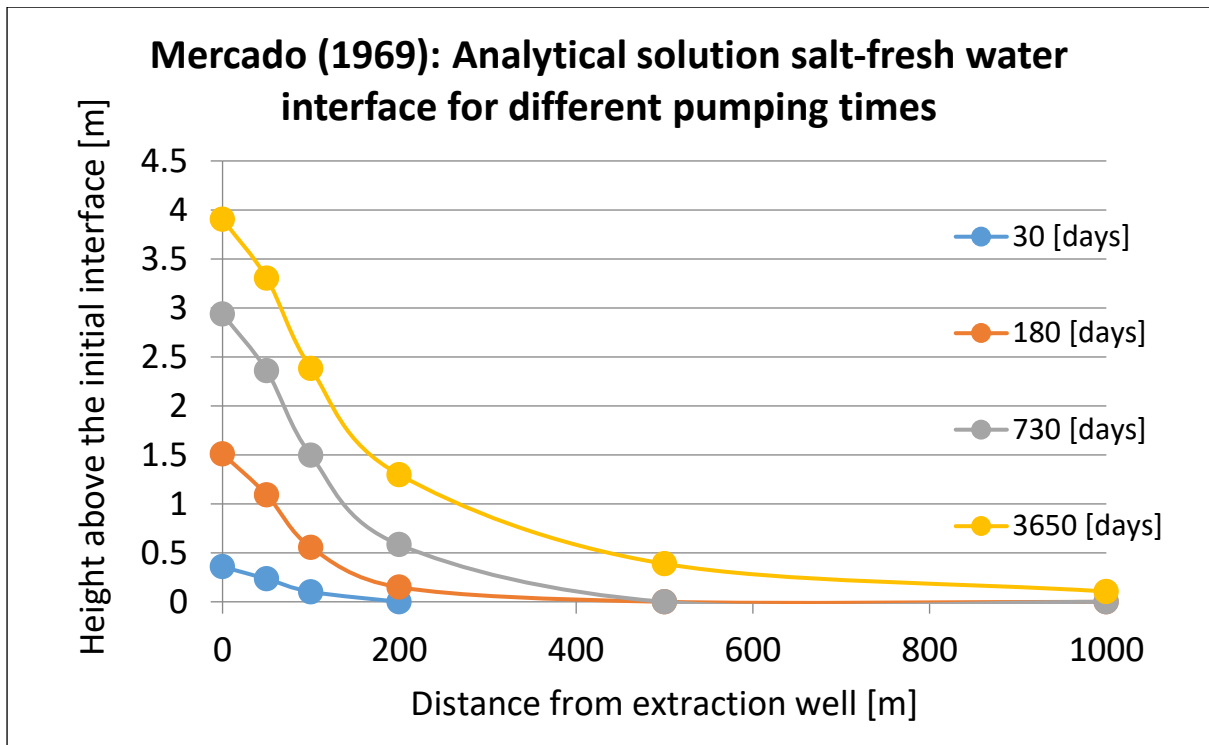


Figure 3.16: Rise of the salt-fresh water interface for different pumping times for the default scenario according to the formula of Mercado (1969). As time progresses, the interface rises vertically, and expands laterally. However, the interface remains at a certain critical height, determined at 4,2 [m]. According to Mercado (1969), a balance is found between the upwards force of the extraction well and the downward force of the gravity. Diluted saline water, however, is able to rise much higher, as shown in Figure 3.17.

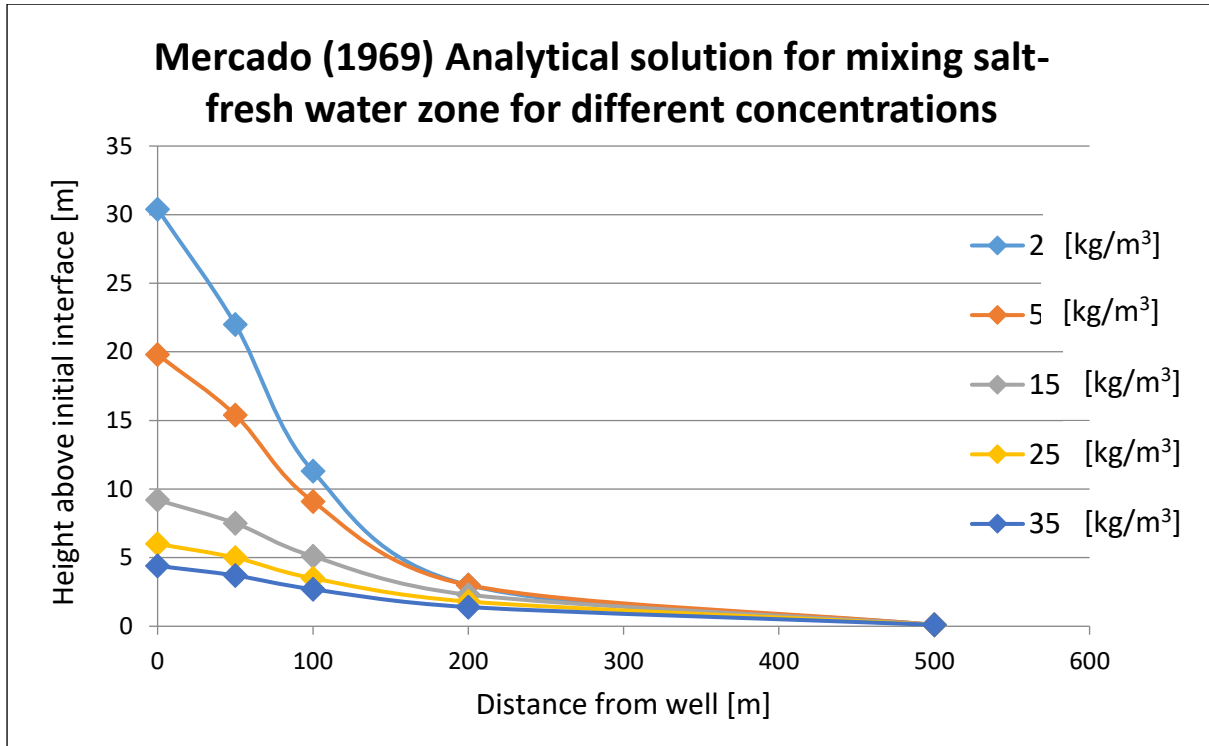


Figure 3.17: Visualization of mixing zone for different concentrations according to the formula of Mercado (1969), when correcting for different densities. Pumping time was set to 10 years and extraction rate was 400 [m³/day] (Scenario 1f). Salt concentration was varied from 35 [kg/m³] (salt-fresh water interface) to 2 [kg/m³] (smallest significant concentration). The lower the concentration difference, the higher the iso-concentration curve gets. The mixing zone becomes almost 30 meters thick after 10 years, while the salt-fresh water interface only becomes 4,2 meters thick.

3.3.3 Analytical solution of Dagan and Bear (1968)

Dagan and Bear (1968) derived a solution for the upconing of a salt-fresh water interface. For saline water upconing, they presented the following equation for the rise of the cone below the extraction well, as described by Diersch et al. (1983).

$$h(t) = \frac{Q * \rho_f}{\sqrt{2\pi(\rho_s - \rho_f)k_r k_z}} * \int_0^{\infty} \frac{\cosh(\lambda(D - L))}{\sinh(\lambda D)} * \left(1 - e^{\frac{-\lambda k_z (\rho_s - \rho_f) t}{n_e (\rho_f \coth(\lambda D) + \rho_s \coth(\lambda S))}} \right) d\lambda$$

Equation (3.6)

This formula is able to predict the rise of the salt cone. Usually, this method is used for the vertical rise of the abrupt salt-fresh water interface. Thus, again we need to adjust for the density difference to mimic a situation where a mixing zone is present. We will use a density difference of 2 [kg/m³], for this is the minimum significant concentration that was determined. Diersch et al. (1983) proposed another simplified version of this formula, for an infinitely thick salt layer. Its results, in combination with results of Mercado (1969) and SEAWAT2000 V4 modeled results, will be shown in Figure 3.18. It is clearly visible that for pumping times shorter than 5 years, results of SEAWAT2000 v4 and Dagan & Bear (1968) match relatively well. Dagan & Bear's method for an infinitely thick salt layer hugely overestimates upconing

compared to every other model. This is probably the result of the infinite amount of available salt in this scenario. This has been explained in section 3.2.5. Section 4.1 will compare these results to other modeled results.

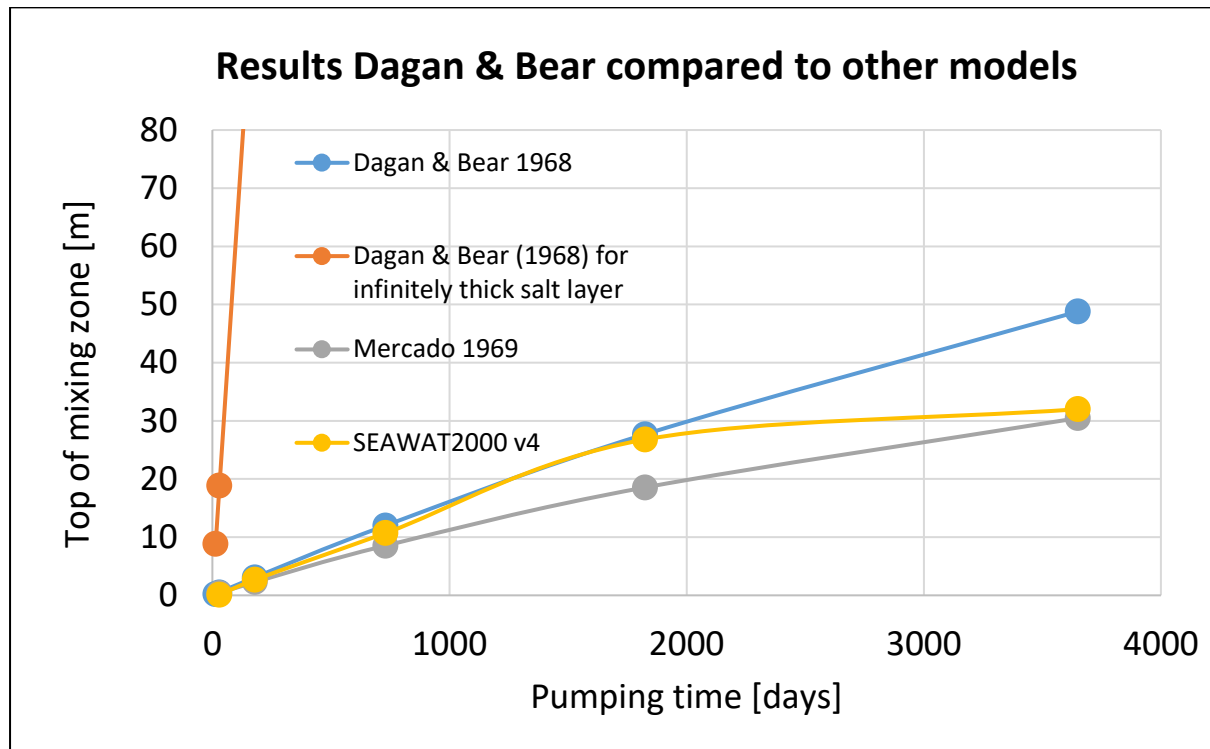


Figure 3.18: Maximum amount of rise of the salt cone for both analytical and numerical solutions. The results of the SEAWAT2000 v4 calculations match best to the analytical solution of Dagan & Bear (1968). This method, however, does not take the maximum height of the aquifer in consideration when calculating the top of the mixing zone, leading to a salt cone height which is higher than the thickness of the aquifer. This is a result of that the initial equation (3.6) calculates the rise of the abrupt interface, instead of the rise of the mixing zone.

4. Conclusion

4.1 Summary different models

In conclusion, we can state that there are many methods available to predict saline water upconing beneath an extraction well. Figure 4.1 shows the results of all relevant numerical and analytical models for the default scenario. None of the model results exactly resemble the numerical model of SEAWAT2000 v4, but all of the models produce results in the same order of magnitude. The analytical solution of Dagan and Bear (1968) produces better results than that of Mercado (1969), but Dagan & Bear's method does not consider that the top of the mixing zone cannot surpass the height of the aquifer. The radial flow equation is too simple and cannot be used for this calculation. Figure 4.2 shows these results for the first year of pumping.

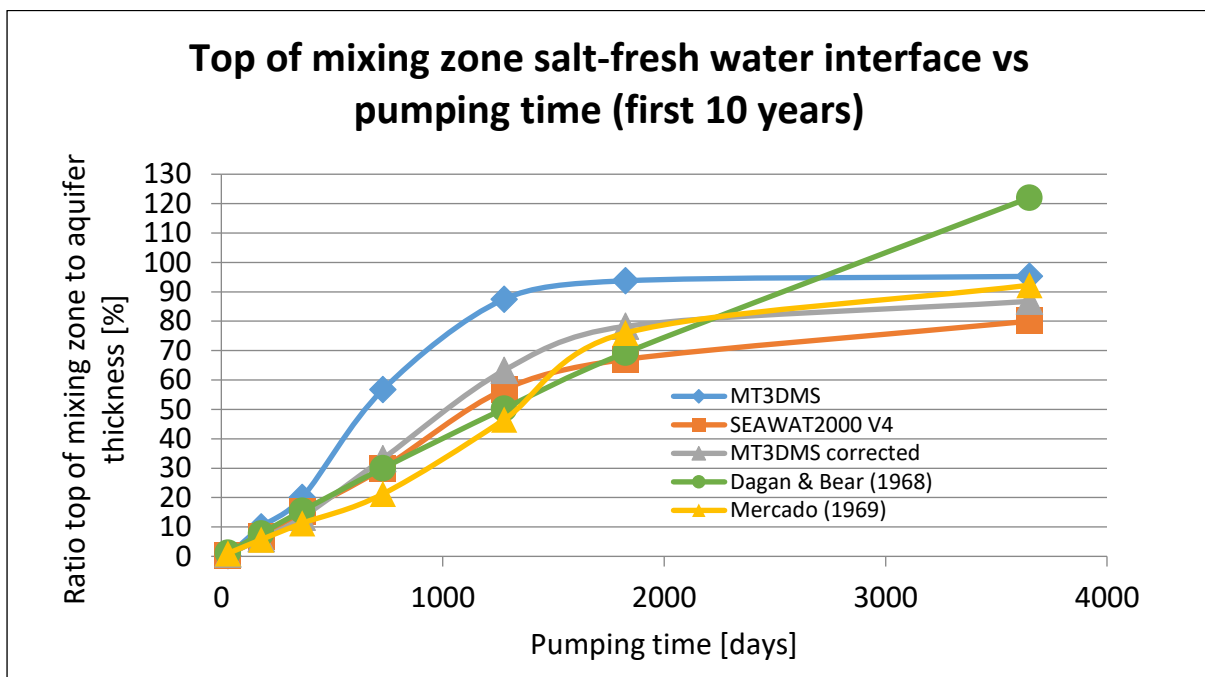


Figure 4.1: Comparison of different methods to calculate the amount of saline water upconing beneath the extraction well for the default scenario (Scenario 1c). MT3DMS tracer transport results produce the highest amounts of upconing (except for $t > 5$ years). Density-dependent model results of SEAWAT2000 V4 produce lower amounts of saline water rise, and the analytical approach of Mercado (1969) produces lowest results. The analytical method of Dagan & Bear (1968) produces results that are closest to that of SEAWAT2000 v4. An S-shape in the graph is somewhat visible for the MT3DMS results. At pumping times smaller than 500 days, results from all three scenarios resemble each other. After 3,5 years of pumping, results differ most per scenario and after 10 years model results converge again, except for the results of Dagan & Bear (1968). For this scenario, the top of the mixing zone rises above the thickness of the aquifer (Figure 3.18), meaning concentrations at the top of the aquifer are higher than $2 \text{ [kg/m}^3\text{]}$.

Considering the results of the sensitivity analysis, it was concluded that the variables that influence the model the most are the state variables: time and space. **The pumping time, pumping rate and thickness of the aquifer** are most crucial to determine the amount of salt upconing (section 3.1.2), in combination with **the amount of available salt** (section 3.2.5). The parameters that were intrinsic to the

characteristics of the aquifer, did not influence the results as strongly as the state variables, time and space. However, of these parameters, the **vertical hydraulic conductivity** had the most influence on the model results the most. Therefore, it is important to acquire a correct representative value for this parameter. Also, the **dispersivity** was an important factor (section 3.4). Since the numerical dispersivity was higher than the physical dispersivity, this results in a **slight overestimation** of all modeled results. This can be considered to be an extra safety factor when applying the numerical models.

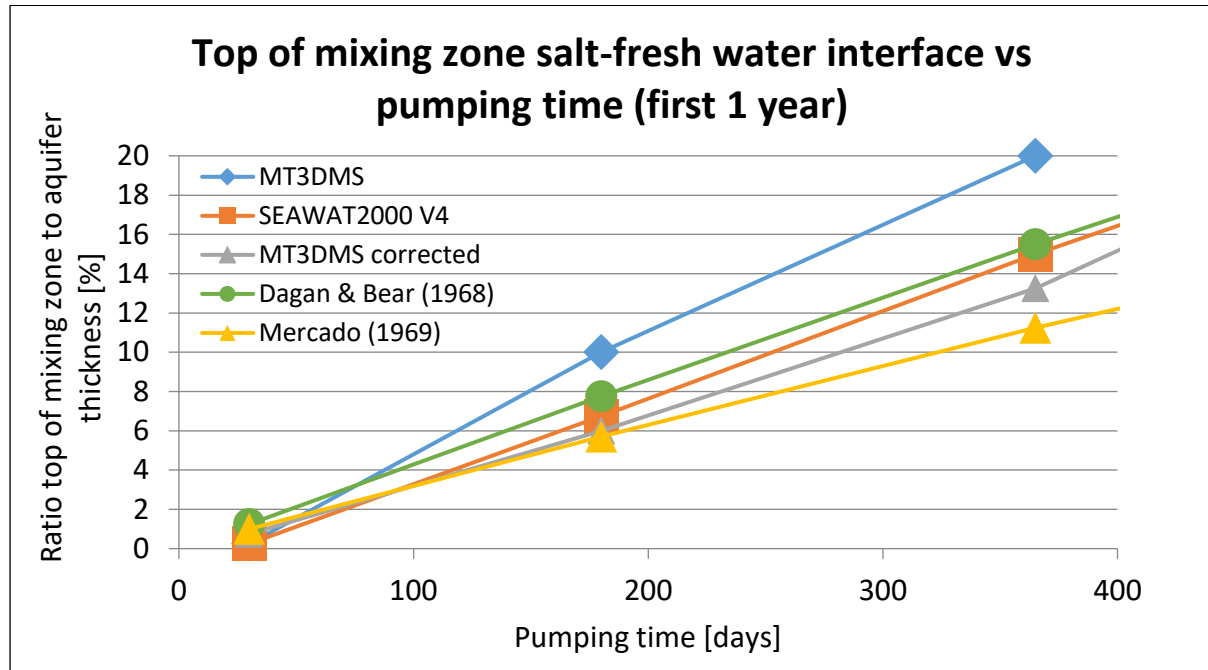


Figure 4.2: Version of Figure 4.1 for shorter pumping times. All methods produce roughly the same extent of vertical rise, with MT3DMS overestimating salt upconing most, and Mercado (1969) underestimating salt upconing most. In this time frame, it is visible that the results of MT3DMS corrected are lower than that of SEAWAT2000 v4.

The research question of this report was: **What is the best method to determine the extent of saline water upconing beneath an extraction well?**

We can answer this question in two ways: If you want the most detailed and advanced method, you could use the **numerical model SEAWAT2000 v4**. Chapter 2: methodology describes how to use this correctly. If you first want to assess quickly if saline water upconing is a possibility, you can run the numerical model MT3DMS. If the results of MT3DMS show that there is a risk of saline water upconing, this report describes three possible methods to quantify this risk. The first option is to switch to the numerically advanced method of SEAWAT2000 v4. The other option is to keep using the MT3DMS model, but to apply one of two correction factors to the results. This correction factor can either be acquired by a **quick method** or a **more accurate method**. The more accurate method is described in section 3.2.3, and the quick method is described in section 4.2. The more accurate method still involves the necessity to run SEAWAT2000 v4 for determining a fitting sorption coefficient. Therefore, this method benefits a user, if multiple simulations need to be done, but one wants to save computational time.

We can compare the importance of the **two main processes** on the amount of upconing; (1) dispersion that leads to a mixing zone and (2) the role of density-driven flow. Both processes have opposing effects on the amount of upconing. Applying density-dependent flow corrections, leads to heavier saline water

that “pulls” the upconing downwards. Opposed to this, the physical and numerical dispersion will lead to increased reach of the salt cone upwards, towards the extraction well. As shown in Figure 4.1 and 4.2, the role of density-dependent flow is significant. The density-dependent model SEAWAT2000 v4 produces results that are averagely at 75% of the results of MT3DMS. When the upconing is halfway of the to be covered distance to the surface, this percentage drops to about 50% (Figure 4.1). As the cone almost reaches the surface this percentage rises to about 80% again. Dispersion turned out to be even more important for the amount of upconing. During upconing, the mixing zone becomes thicker and thicker, until it reaches the well. This will lead to the extraction of saline water, when the salt-fresh water interface is still deeper in the surface. This mixing zone can reach a factor 6-7 higher than the salt-fresh interface reaches (Figure 3.17). Therefore, it can be concluded that dispersion has a greater impact on upconing than the role of density-dependent flow has.

4.2 Practical applications

If we imagine a theoretical large-scale dewatering operation. What are the practical steps to take to ensure that no significant salinization reaches the surface?

First, the hydrogeological system needs to be mapped. What are the dimensions of the to be dewatered volume and what is the thickness of the aquifer until saline water is reached? A vertical concentration profile should be made to map the initial salinity as best as possible. Then, other parameters of the aquifer should be determined, most importantly: hydraulic conductivity (horizontal and vertical) and porosity.

If the situation is mapped, we can choose one of the described methods to calculate the amount of saline water upconing. It is advised to use either the MT3DMS tracer transport method or the density-dependent SEAWAT2000 v4 method, inside a MODFLOW model like Groundwater Vistas Version 7.19.

Then, we need to create a representative model using all our acquired input parameters. The only variables we are able to control is the **pumping time** and the **pumping rate**. Thus, we need to run the model with different values of pumping time and pumping rate to model the effect of saline water upconing. The best model to use is that of SEAWAT2000 v4, as explained above. This model, however, is computationally heavy. So, when we do not have the time to run SEAWAT2000 v4, we could use the tracer transport model MT3DMS.

If we run the MT3DMS model, we can choose for the **quick method** or the **more accurate method**. The more accurate method predicts saline water upconing as if it was slowed down by a chemical reaction (adsorption). This can be modeled by determining the best fitting value of the sorption coefficient (explained in section 3.2.2). The quick method just takes the MT3DMS calculation and puts the amount of upconing averagely at a **factor 0,75** of that. This corrected curve is visualized in Figure 4.3. Unfortunately, this method is not physically based, and thus, can only be used as an indication. Nonetheless, its results match the results of SEAWAT2000 v4 quite well, especially during the first year of pumping (Figure 4.3).

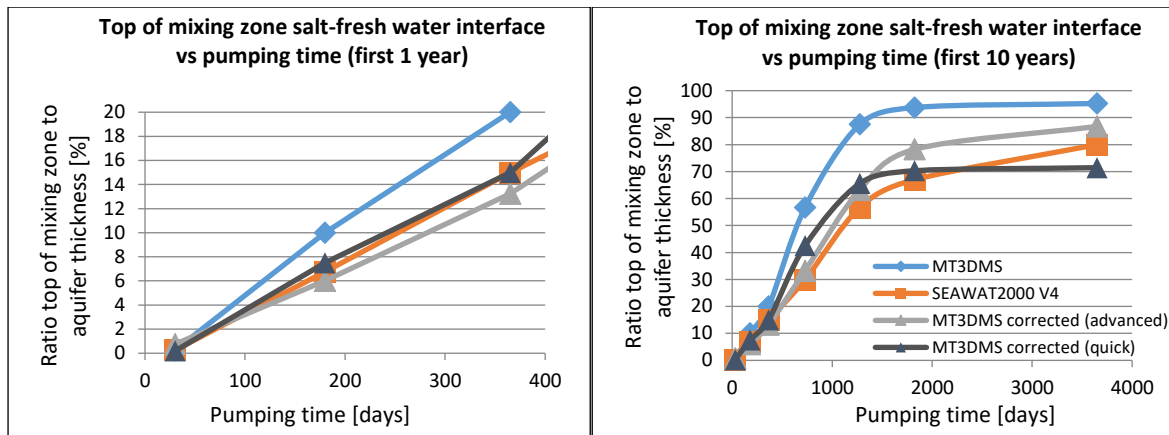


Figure 4.3: Version of Figure 4.1 and 4.2, with the quick correction method (dark grey). Especially during the first year of pumping, the quick method produces results that resemble the results of SEAWAT2000 v4 very well. The quick method curve takes the result of MT3DMS and multiplies it by a factor of 0,75.

Using this quick method, a lot of time can be spared to assess if there is a risk of salinization of the subsurface. If the risk turns out to be substantial, one of the more accurate models should be used to correctly predict saline water upconing.

4.3 Recommendations

We need to take a few important considerations, when applying the techniques described in this report.

First of all, this entire model is based on a situation where dewatering is a result of **single source extraction**. There is only one pumping well that accounts for all of the dewatering. During most dewatering projects, multiple extraction wells are used to even out the effects of lowering groundwater levels and rising saline water. This would allow a much larger available pumping rate for the system. This is useful, since for most calculations in this report a pumping rate of 400 [m³/day] was used. This is substantially lower than the pumping rates of wells used in large-scale dewatering projects. For example, during the Hyde park dewatering operation in Hoofddorp, a total volume of 4.000.000 [m³] of water will be extracted for a period of 4 years. This extraction is distributed over multiple pumping wells that will extract 100 [m³/hour]. This extraction rate is much larger than the pumping rate used in this research. Further research could investigate the effects of rising saline water as result of multi-source extraction.

Also, it is important to realize what happens with the extracted water. In most cases, this is **re-injected** back in the aquifer. As this water has strongly diluted concentrations of salt (section 3.2.4), this would affect the salt concentration of the aquifer. When this water is reinjected near the salt cone, complicated flow patterns would arise. It is possible that the injection of this water reduces the salt concentration of the cone. Another modelling study could assess the consequences of this phenomenon.

A third point of attention is the lack of an initial mixing zone. In all calculations, there was initially a **sharp interface of fresh and salt water**. This was done because the thickness of the mixing zone varies per location (H. Diersch et al., 1983). Therefore, the mixing zone was set be absent in the initial default scenario. When applying the methods described in this report, one should take in mind that a correct and representative depth-concentration profile should be used. This can be done in a field study, using a multi-depth concentration sampler.

The fourth point of attention assesses the **numerical dispersion** of the model. This numerical dispersion is model-inherent and affects the rise of the saline water cone. Section 6.2 quantifies this numerical dispersion and describes how this leads to a slight overestimation of the results. If we increase the resolution of the model, the numerical dispersion decreases, but it will not be zero. Thus, if a user wants to apply this model, he would need to use a sufficiently small grid size. To determine whether a grid resolution is good enough, the analysis in section 6.2 can be used.

The last insight that we should assess is the **depth of the extraction well**. In most scenarios, the extraction well was placed just below the surface. If we apply a fully penetrating well, we can place the extraction well at the same depth as the saline water. As explained in section 3.1.1, the saline water will not reach the parts of the aquifer above the extraction well. This would solve the problem of upconing, but the extracted water will still be very saline. Thus, re-injection should be done at the same depth, or else the re-injected water could still cause salinization of other parts of the aquifer. We would expect only a lateral migration of saline water in this scenario. However, further research could assess the precise effects of the re-injection.

References

- Bakker, M. (2003). A Dupuit formulation for modeling seawater intrusion in regional aquifer systems. *Water Resources Research*, 39(5).
- Barlow, P. M., & Reichard, E. G. (2010). Saltwater intrusion in coastal regions of North America. *Hydrogeology Journal*, 18(1), 247-260.
- Bear, J., Cheng, A. H. D., Sorek, S., Ouazar, D., & Herrera, I. (Eds.). (1999). *Seawater intrusion in coastal aquifers: concepts, methods and practices* (Vol. 14). Springer Science & Business Media.
- Bedekar, V., Morway, E. D., Langevin, C. D., & Tonkin, M. J. (2016). MT3D-USGS version 1: A US Geological Survey release of MT3DMS updated with new and expanded transport capabilities for use with MODFLOW (No. 6-A53). US Geological Survey.
- Cai, J., Taute, T., & Schneider, M. (2014). Saltwater upconing below a pumping well in an inland aquifer: a theoretical modeling study on testing different scenarios of deep saline-groundwater pathways. *Water, Air, & Soil Pollution*, 225(11), 2203.
- Christelis, V., & Mantoglou, A. (2018). Pumping Optimization of Coastal Aquifers Using Seawater Intrusion Models of Variable-Fidelity and Evolutionary Algorithms. *Water Resources Management*, 1-14.
- Custodio, E. (2010). Coastal aquifers of Europe: an overview. *Hydrogeology Journal*, 18(1), 269-280.
- Dagan, G., & Bear, J. (1968). Solving the problem of local interface upconing in a coastal aquifer by the method of small perturbations. *Journal of hydraulic research*, 6(1), 15-44.
- De Lange, W. J., Prinsen, G. F., Hoogewoud, J. C., Veldhuizen, A. A., Verkaik, J., Essink, G. H. O., ... & Kroon, T. (2014). An operational, multi-scale, multi-model system for consensus-based, integrated water management and policy analysis: The Netherlands Hydrological Instrument. *Environmental Modelling & Software*, 59, 98-108.
- De Louw, P. G. B., Vandenbohede, A., Werner, A. D., & Essink, G. O. (2013). Natural saltwater upconing by preferential groundwater discharge through boils. *Journal of Hydrology*, 490, 74-87.
- Dehaan, R. L., & Taylor, G. R. (2002). Field-derived spectra of salinized soils and vegetation as indicators of irrigation-induced soil salinization. *Remote sensing of Environment*, 80(3), 406-417.
- Diersch, H. J. (1983). On finite element upwinding and its numerical performance in simulating coupled convective transport processes. *ZAMM-Journal of Applied Mathematics and Mechanics/Zeitschrift für Angewandte Mathematik und Mechanik*, 63(10), 479-488.
- Diersch, H. J., & Kolditz, O. (2002). Variable-density flow and transport in porous media: approaches and challenges. *Advances in water resources*, 25(8-12), 899-944.
- Egorov, A. G., Demidov, D. E., & Schotting, R. J. (2005). On the interaction between gravity forces and dispersive brine fronts in micro-heterogeneous porous media. *Advances in water resources*, 28(1), 55-68.

- Essink, G. O. (2001). Saltwater intrusion in 3D large-scale aquifers: a Dutch case. *Physics and Chemistry of the Earth, Part B: Hydrology, Oceans and Atmosphere*, 26(4), 337-344.
- Freijer, J. I., Veling, E. J. M., & Hassanizadeh, S. M. (1998). Analytical solutions of the convection–dispersion equation applied to transport of pesticides in soil columns. *Environmental modelling & software*, 13(2), 139-149.
- Fitts, C. R. (2002). *Groundwater science*. Elsevier.
- Giambastiani, B. M., Antonellini, M., Essink, G. H. O., & Stuurman, R. J. (2007). Saltwater intrusion in the unconfined coastal aquifer of Ravenna (Italy): a numerical model. *Journal of Hydrology*, 340(1-2), 91-104.
- GUIDE, G. S. (2011). *Visual Modflow*
- Guo, W., & Bennett, G. D. (1998). Simulation of saline/fresh water flows using MODFLOW. In *Proceedings of MODFLOW '98 conference at the international ground water modeling center, Colorado School of Mines, Golden, Colorado (Vol. 1, pp. 267-274)*.
- Guo, W., & Langevin, C. D. (2002). User's guide to SEAWAT; a computer program for simulation of three-dimensional variable-density ground-water flow (No. 06-A7).
- Harbaugh, A. W., Banta, E. R., Hill, M. C., & McDonald, M. G. (2000). MODFLOW-2000, The U. S. Geological Survey Modular Ground-Water Model-User Guide to Modularization Concepts and the Ground-Water Flow Process. Open-file Report. U. S. Geological Survey, (92), 134.
- Henry, H.R., 1964. Effects of dispersion on salt encroachment in coastal aquifers. In: *Sea Water in Coastal Aquifers, US Geol. Surv. Supply Pap. 1613-C*, pp. 70–84.
- Kipp Jr, K. L., & HST3D, A. (1986). A computer code for the simulation of heat and solute transport in three-dimensional groundwater flow systems. *US Geol. Surv. Water Resour. Invest. Rep*, 86-4905.
- Konikow, L. F., Goode, D. J., & Hornberger, G. Z. (1996). A three-dimensional method-of-characteristics solute-transport model (MOC3D) (pp. 96-4267). US Geological Survey.
- Landman, A. J., Johannsen, K., & Schotting, R. (2007). Density-dependent dispersion in heterogeneous porous media Part I: A numerical study. *Advances in water resources*, 30(12), 2467-2480.
- Langevin, C. D. (2009). SEAWAT: A computer program for simulation of variable-density groundwater flow and multi-species solute and heat transport (No. 2009-3047). US Geological Survey.
- Langevin, C. D., & Guo, W. (2006). MODFLOW/MT3DMS–Based Simulation of Variable-Density Ground Water Flow and Transport. *Groundwater*, 44(3), 339-351.
- Langevin, C. D., Essink, G. O., Panday, S., Bakker, M., Prommer, H., Swain, E. D., ... & Barcelo, M. (2004). MODFLOW-based tools for simulation of variable-density groundwater flow. Boca Raton, FL: Lewis Publishers.
- Langevin, C. D., Thorne Jr, D. T., Dausman, A. M., Sukop, M. C., & Guo, W. (2008). SEAWAT version 4: a computer program for simulation of multi-species solute and heat transport (No. 6-A22). Geological Survey (US).

- Lebbe, L. (1983). Mathematical model of the evolution of the fresh water lens under the dunes and beach with semi-diurnal tides. *Geologia applicata e idrogeologia*, 18(2), 211-226.
- McDonald, M. G., & Harbaugh, A. W. (1988). A modular three-dimensional finite-difference groundwater flow model (Vol. 6, p. A1). Reston, VA: US Geological Survey.
- Mercado, A. et al. (1969). Upconing of fresh water—sea water interface below pumping wells, field study. *Water Resources Research*, 5(6), 1290-1311.
- Olsthorn, T. N. (2000). Brackish-saline water movement in the southern part of the Amsterdam Dune Water Area, 1925-2025. In *Proceedings of the 16th Salt Water Intrusion Meeting-SWIM* (pp. 119-126).
- Oude Essink, G. (1998). MOC3D adapted to simulate 3D density-dependent groundwater flow. In *Proceedings of the MODFLOW'98 Conference* (pp. 291-303). Gerven and Schaars (1998)
- Post, V. E. A. (2005). Fresh and saline groundwater interaction in coastal aquifers: is our technology ready for the problems ahead?. *Hydrogeology Journal*, 13(1), 120-123.
- Polemio, M., & Romanazzi, A. (2012). Modelling and groundwater management of a karstic coastal aquifer: the case of Salento (Apulia, Italy). 22nd SWIM.
- Powers, J. P., Corwin, A. B., Schmall, P. C., & Kaeck, W. E. (2007). *Construction dewatering and groundwater control: new methods and applications*. John Wiley & Sons.
- Puller, M. (2003). *Deep excavations: a practical manual*. Thomas Telford.
- Praveena, S. M., & Aris, A. Z. (2010). Groundwater resources assessment using numerical model: A case study in low-lying coastal area. *International Journal of Environmental Science & Technology*, 7(1), 135-146.
- Ranjan, P., Kazama, S., & Sawamoto, M. (2006). Effects of climate change on coastal fresh groundwater resources. *Global Environmental Change*, 16(4), 388-399.
- Rumbaugh, J.O., and D.B. Rumbaugh. 2017. *Groundwater Vistas Version 7 Manual*. Leesport, Pennsylvania: Environmental Simulations Inc.
- Scott, R. A., & Daw, G. P. (1983). Ground water pressure relief wells in shaft sinking. *International Journal of Mining Engineering*, 1(3), 229-236.
- Segol, G. (1994). *Classic groundwater simulations: proving and improving numerical models*. Prentice Hall.
- Simmons, C. T. (2005). Variable density groundwater flow: From current challenges to future possibilities. *Hydrogeology Journal*, 13(1), 116-119.
- Simmons, C. T., Fenstemaker, T. R., & Sharp Jr, J. M. (2001). Variable-density groundwater flow and solute transport in heterogeneous porous media: approaches, resolutions and future challenges. *Journal of Contaminant Hydrology*, 52(1-4), 245-275.
- Sorek, S., & Pinder, G. F. (1999). Survey of computer codes and case histories. In *Seawater Intrusion in Coastal Aquifers—Concepts, Methods and Practices* (pp. 399-461). Springer, Dordrecht.

Van Ommen, H. C., et al. "Experimental assessment of preferential flow paths in a field soil." *Journal of Hydrology* 105.3-4 (1989): 253-262.

Voss, C. I., & Provost, A. M. (1984). Sutra. US Geological Survey Water Resources Investigation Reports, 84-4369. Voss and Provost 2002)

Wagner J. & Kent D. C. (1985) Upconing of a salt-water/fresh-water interface below a pumping well. Robert S. Kerr Environmental Research Laboratory - Oklahoma State University EPA/600/2-85/066

Zheng, C. (1990). {MT3D}, A modular three-dimensional transport model.

Zheng, C., & Wang, P. P. (1999). MT3DMS: a modular three-dimensional multispecies transport model for simulation of advection, dispersion, and chemical reactions of contaminants in groundwater systems; documentation and user's guide. Alabama Univ University.

Zheng, C., & Wang, P. P. (1999). MT3DMS: a modular three-dimensional multispecies transport model for simulation of advection, dispersion, and chemical reactions of contaminants in groundwater systems; documentation and user's guide. Alabama Univ University.

Zuurbier, K. G., Zaadnoordijk, W. J., & Stuyfzand, P. J. (2014). How multiple partially penetrating wells improve the freshwater recovery of coastal aquifer storage and recovery (ASR) systems: A field and modeling study. *Journal of hydrology*, 509, 430-441.

6. Appendix

6.1 Model validation: The Henry problem

The Henry saltwater intrusion problem (Henry, 1964) is considered the standard analysis for testing density-driven groundwater flow models (Guo & Langevin, 2002). The setup consists of a cross-section of a confined aquifer, which is homogeneous and isotropic. A constant flux of freshwater is set to the inland boundary condition (left); while a saline water boundary condition (right) is set to a constant concentration boundary of saline seawater. Henry (1964) established a semi-analytical explanation for the steady-state spreading of salt concentration in the setup.

Since an analytical solution existed for the Henry problem, lots of numerical codes have been developed and evaluated to this Henry solution (Guo & Langevin, 2002). Segol (1994) exposed, however, that the Henry solution was not entirely correct, since Henry (1964) removed, for computational reasons, mathematical terms from the equations that he believed to be irrelevant. Segol (1994) recalculated the original solution with the initially removed terms and the new answer was somewhat different from Henry's result. Segol (1994) developed a new numerical code: the SUTRA code and he was able to reproduce the accurate solution for the Henry problem (Guo & Langevin, 2002).

The User's guide to SEAWAT (Guo & Langevin, 2002) provides the correct steady-state concentration profile of the problem and is shown in Figure 6.1. The solution shows the contours of relative concentration in percent, calculated from the SUTRA code (Segol, 1994). Table 2.2 provides the hydrogeological and numerical parameters used to create these results.

Parameter	value
Model size	2 [m] long, 1 [m] high, and 1 [m] wide
Grid size	0,1 x 0,1 x 1 [m]
Inflow (Q)	5.702 [m ³ /day]
Hydraulic conductivity (k)	864 [m/day]
Dispersivity (long + trans) ($\alpha_L = \alpha_t$)	0 [m]
Molecular diffusion (D_m)	1.62925 [m ² /day]
Seawater concentration (C_s)	35 [kg/m ³]
Time settings	1 [day]; 23 time steps; 1,9 time step multiplier

Table 6.1: Input parameters Henry problem.

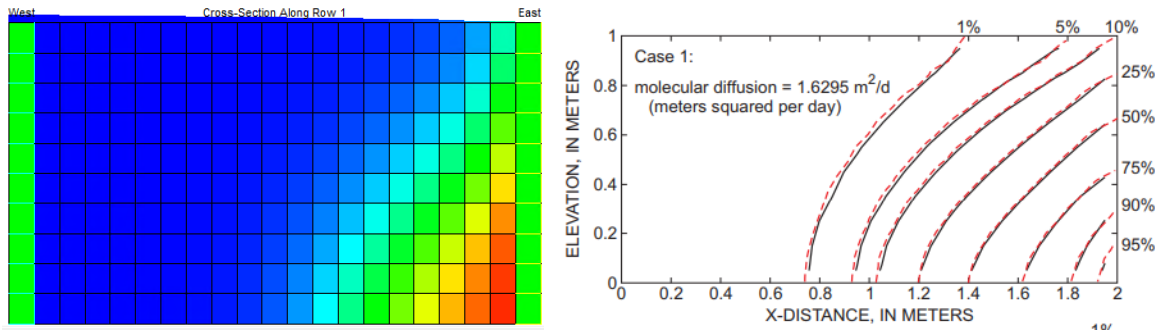


Figure 6.1: *Left: Color contour plot of the steady-state concentration distribution modeled by SEAWAT2000 V4 on GWVistas. The red color represents a concentration of 35 [kg/m³] and the blue color represents a concentration of 0 [kg/m³]. Right: Contours of relative concentration in percent, calculated from the SUTRA code (Segol, 1994), provided in the User's guide to SEAWAT (Guo & Langevin, 2002)*

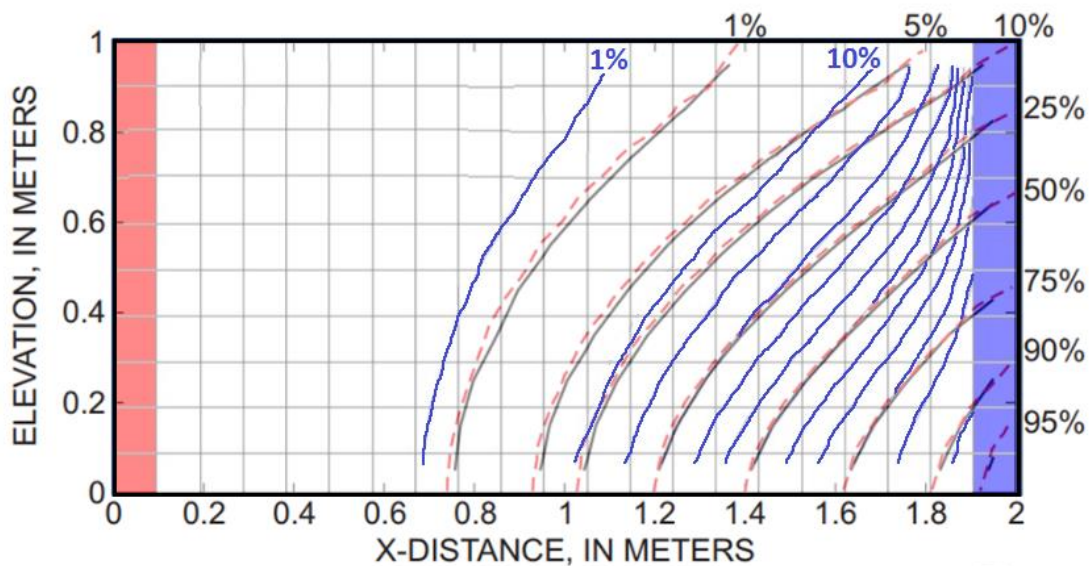


Figure 6.2: *Results from SEAWAT2000 V4 (blue) overlain over results calculated from the SUTRA code (Segol, 1994) (black & red), provided in the User's guide to SEAWAT (Guo & Langevin, 2002). Blue contours match relatively well, slight variations may be caused by a difference in unspecified numerical values of MODFLOW and MT3DMS.*

6.2 Determining numerical dispersion

There are two types of dispersion that influence the modeled results. The first one is physical dispersion and the second one is numerical dispersion. The physical dispersion has been discussed in section 3.1. The numerical dispersion is model-inherent and is governed by the technique the numerical solution scheme solves the model equations per grid cell. The solution scheme used for the MT3DMS model is the finite difference method. When this method is used, all terms in the governing equation are treated simultaneously, with all advection, dispersion, reactions, and sink/source terms represented with finite-difference approximations. This means that all terms are represented with implicit-in-time weighted finite-difference approximations (GUIDE, G. S. (2011). Visual Modflow).

Other solution schemes (MOC, MMOC, and HMOC) are particle-based methods. When the particle-based methods or the TVD (higher-order finite-volume) method are selected to simulate solute transport, the transport equation is split into two parts. The HMOC method combines the MOC and the MMOC methods by using an automatic adaptive scheme that uses the MOC technique at sharp concentration fronts, and the MMOC method away from the fronts. Thus, the HMOC scheme can provide accurate solutions for both sharp and non-sharp front problems (GUIDE, G. S. (2011). Visual Modflow). Since this method is particle-based, numerical dispersion can be considered to be negligible. Thus, if we compare the results of the HMOC solution scheme to the results of the Finite Difference solution scheme, we can compare the degree of numerical dispersion.

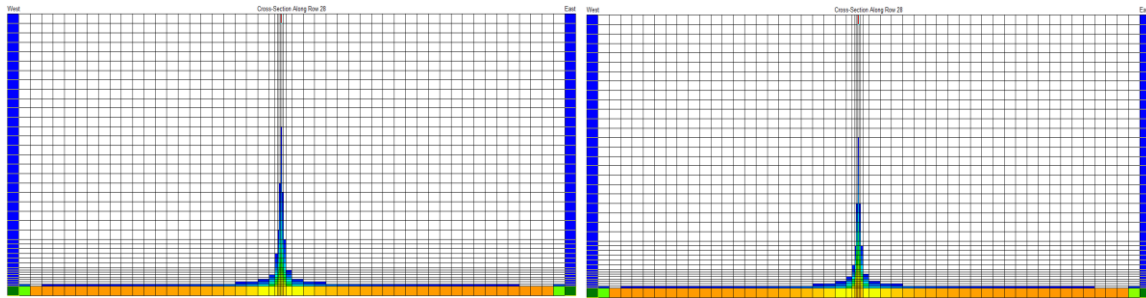


Figure 6.3: *left:* Salt upconing when modeled with the finite difference solution method. *right:* Salt upconing when modeled with the HMOC solution method. Both cross-sections show almost the same extent of upconing.

Solution scheme (scenario 1d, 2 years)	Top of mixing zone [m]
HMOC (particle-based)	21,3
Finite difference method	22,7
Relative difference	6,2%

Table 6.2: Results numerical dispersion quantification analysis.

Comparing the results of the HMOC solution method and the finite difference method, we see that the finite difference method provides a salt cone that reaches a little bit higher (22,7 m). It is reasonable to state that the difference between the two results is caused by the numerical dispersion effect which occurs in the finite difference analysis. Thus, the numerical dispersion can be considered to 6,2% for the MT3DMS model.

To exactly **quantify the numerical dispersion** that is present in the model, we performed the following analysis.

We take our default model, put physical dispersivity to zero, and we replace the layer with an initial concentration of 0 [kg/m³] for a constant concentration layer of 1 [kg/m³]. Then, we remove the constant head boundaries on the sides, and apply a head gradient of 10 [m] at the bottom of the model and 0 [m] at the top of the model. This allows for an upward flow of concentration, in which the solute will disperse. This dispersion is visualized by the orange data points in Figure 6.4.

If we want to know which value of dispersivity (α), results in such a behavior, we need to fit these results to the analytical solution of one-dimensional dispersion in a homogeneous porous medium.

We can use the formula of Freijer & Hassanizadeh (1998) for one-dimensional dispersion in a semi-infinite medium for this calculation.

$$C(x, t) = \frac{1}{2} C_0 * \left[\operatorname{erfc} \left(\frac{x - vt}{2\sqrt{D_x t}} \right) + e^{\frac{xv}{D_x}} \operatorname{erfc} \left(\frac{x + vt}{2\sqrt{D_x t}} \right) \right]$$

Where:

$$v = \frac{q}{n_e} \quad \text{and} \quad D_x = \alpha * v \quad \text{and} \quad q = k \frac{dh}{dx}$$

In this formula, water velocity is represented by (v), the dispersion coefficient is represented by (D_x), and the vertical distance from the initial interface is represented by (x). If we want to fit the results of this equation to the data points of our model, we need to find a value for the dispersivity (α). The blue data points represent the results best, if we use **α = 2,3 [m]**. This value of dispersivity fits best to our default model. Since the physical dispersivity of the model was set to zero, we can conclude that the remaining dispersion is a result of the numerical dispersivity. Thus, the numerical dispersivity can be quantified to be 2,3 [m]. In our default model, we use a physical dispersivity of 1 [m]. We can thus conclude that the total dispersivity in the default model is 3,2 [m].

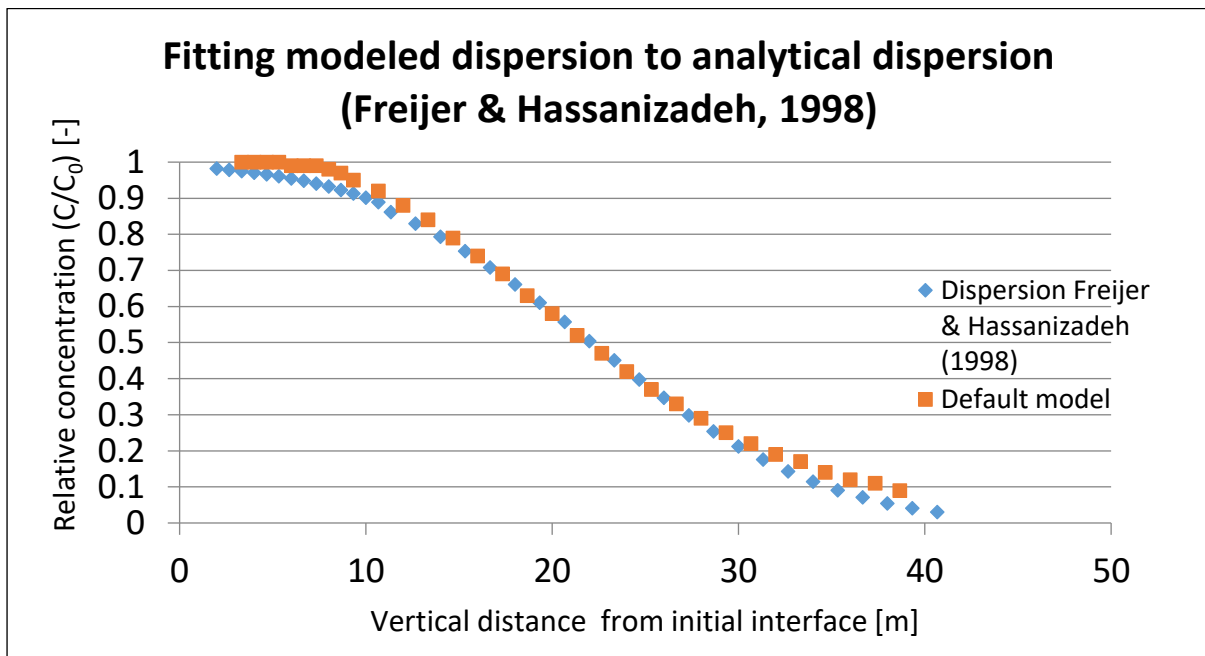


Figure 6.4: Two breakthrough curves of relative solute concentration vs distance. The orange data points represent the results of the model, and the blue data points represent the results of the analytical solution of Freijer & Hassanizadeh (1998).

Also, we can conclude that the numerical dispersivity is higher than the physical dispersivity. This means that most of the dispersion is model-inherent. If we want to decrease this numerical dispersivity, we can increase the resolution of the grid. If we run the model with twice as many layers (changing 39 layers to 78 layers), we will find that less numerical dispersion occurs. The alpha value was found to be **1,9 [m]**. This means that increasing the grid size leads to less numerical dispersion, but the difference is not very substantial. Also, the computational time increases when using a finer grid.

If the numerical dispersion is higher than the physical dispersion, we know that our modeled results **still** slightly overestimate salt upconing. This slight overestimation can be considered to be an extra safety factor when applying this method for real world scenarios. This numerical “flaw” of the model can thus be an extra safety net for salt upconing calculations.